Long term Drivers of Hydrological change in the Southeastern United States

by

Arshdeep Singh

A thesis submitted to the Graduate Faculty of
Auburn University
in partial fulfillment of the
requirements for the Degree of
Master of Science in Natural Resources

Auburn, Alabama
August 8, 2020

Keywords: climate change, land-use change, water cycle, streamflow trends

Approved by

Dr. Sanjiv Kumar, Chair, Assistant Professor, School of Forestry and Wildlife Sciences
Dr. Latif Kalin, Professor, School of Forestry and Wildlife Sciences
Dr. Danica L. Lombardozzi, Project Scientist II, NCAR, Boulder, CO

Abstract

Plant response to elevated CO_2 concentration is known to increase leaf-level water-use efficiency through a reduction in stomatal opening. Recent studies have emphasized that increased plant water-use efficiency can ameliorate the impact of drought due to climate change. However, there is a potentially counterbalancing impact due to the increased leaf area. We investigate long-term trends (1951 to 2015) of observed streamflow in the Southeastern United States (SE US) and quantify the contribution of major drivers of streamflow changes using single factor climate modeling experiments from Community Land Model Version 5 (CLM5). The SE US streamflow observations do not exhibit a trend, which is in agreement with the CLM5 control experiment. Using the factorial set of CLM5 experiments, we find that increased leaf area under elevated CO_2 leads to decreased runoff and completely counteracts increased runoff due to water-use efficiency gains under elevated CO_2 and land-use change.

Acknowledgments

I give my deepest gratitude to my advisor, Dr. Sanjiv Kumar, for his invaluable guidance and support throughout my graduate studies. I would also like to thank Dr. Latif Kalin and Dr. Danica L. Lombardozzi for their time in my MS committee and offering valuable suggestions. I especially thank Dr. David M. Lawrence for his significant input in land-use change study, and encouragement. I also thank my friends: Recep Tayyip Kanber, Henrique Haas, Junhao He, and Musa Esit for their encouragement and a congenial working environment. I acknowledge the support of USDA Hatch funding #ALA031-1-18023. I thank Yanan Duan for her help in running the trend analysis on Auburn Supercomputer. I acknowledge the computing support from NCAR CISL (Allocation #UAUB0003). The "Stomatal Conductance Constant CO_2" experiment data are available online (DOI:10.5065/GKPE-DK86). The CMIP6 LUMIP model outputs were downloaded from PCMDI/LLNL (California) (https://esgf-node.llnl.gov/projects/cmip6/). I thank the CMIP6-LUMIP modeling groups for providing model outputs. Last but most importantly, I thank my family for their unlimited support during my MS studies, and for their unwavering trust in me.

Table of Contents

List of Tables

List of Figures

List of Abbreviations

AVHRR	Advanced Very High-Resolution Radiometer
CDR	Climate Data Record
CLM5	Community Land Model Version 5
CMIP6	Coupled Model Intercomparison Project phase 6
ENSO	El Niño–Southern Oscillation
ET	Evapotranspiration
FACE	Free Air CO_2 Enrichment
GISS	Goddard Institute for Space Studies
GSWP3	Global Soil Wetness Project Phase 3
H	Hurst coefficient
LAI	Leaf Area Index
LTP	Long-term persistence
LUCC	Land Use/Cover change
LUMIP	Land Use Model Intercomparison Project
NDVI	Normalized Difference Vegetation Index
NOAA	National Oceanic and Atmospheric Administration
SE US	Southeastern United States
TSA	Magnitude of Trend
USGS	United States Geological Survey
WUE	Water use efficiency

Chapter 1. Background and Motivation

1.1 Introduction

Water is mandatory for the survival of humanity. The water falls on ground by the process known as precipitation, in the form of rain, snow etc. This water either enters soil by infiltration or flows as runoff through streams, rivers, etc. The plants uptake water for growth and development and finally losses water in exchange for carbon dioxide by the process known as transpiration (Ukkola et al., 2016). The water that enters soil profile, called soil moisture, influences water and energy balances (Kumar et al., 2020; Livneh & Hoerling, 2016; Misra et al., 2015). Soil moisture content is the key determinant of plant ecosystems and is affected by the climate, land-atmosphere interactions, and vegetation types. If soil moisture is deficient, the water demand of the plants is not fulfilled. Therefore, in recent decades, new modeling approaches to monitor and analyze soil moisture have been developed. These techniques include networks of in-situ observations, remotely sensed soil moisture data, and model-data integration (Crow & Yilmaz, 2014; Quering et al., 2016).

Vegetation distribution and its interaction with the atmosphere affect water and energy balances at the land-surface. The vegetation growth is affected by temperature, precipitation, nutrients, radiation, competition etc. determine the vegetation growth, and in return, vegetation controls water fluxes via evapotranspiration and runoff. The surface albedo and longwave radiation are lower in the vegetated areas than the bare lands because vegetated areas reduce heat loss and increase precipitation compared to bare lands (Charney, 1975). Therefore, vegetation acts as positive land-atmosphere feedback. Human interference has resulted in significant land-use change that has resulted in water availability changes in many parts of United States (Y. K. Zhang & Schilling, 2006; C. Zhu & Li, 2014) and

globally (Gornitz et al., 1997; Wada et al., 2017, 2010). Land use change affects the albedo, thus impacting surface energy balance. Land use change affects how that energy is partitioned into sensible and latent heat fluxes, the turbulent energy fluxes that transfer water and heat into the atmosphere (De Noblet-Ducoudré est al., 2012; Mahmood et al., 2014). found that the impacts of anthropogenic land-use on water availability. (Padrón et al., 2017) found that land use impacts on water availability are smaller than reported in the literature.

The decrease in stomatal conductance is due to fact that there is more CO_2 in the atmosphere, which means that plants do not need their stomata open as much to acquire the CO_2. It results in higher assimilation rates, but the higher assimilation rates themselves are not the cause of the lower stomatal conductance – the elevated CO_2 concentrations are (Forkel et al., 2016). Increasing carbon dioxide concentration in the atmosphere will therefore increase the plant's water use efficiency – the amount of water used to gain carbon – and hence, should increase water availability. Studies have found an increase in water availability with the historical increases in CO_2 concentrations due to CO_2 physiological responses, namely an increase in plant WUE (Kumar et al., 2016; Yang et al., 2018). However, CO_2 fertilization effect can decrease runoff due to increased vegetation. Idso and Kimball (1992) suggested that plant growth increased by 3.8 times due to doubling the CO_2 concentration relative to the present level. Plant growth increase is associated with the CO_2 increase due to higher photosynthetic rate (Donohue et al., 2013) and might decrease water availability. In general, CO_2 is increasing growth in most places, but the effect of temperature is more variable. It increases growth in high latitudes, but not necessarily in low latitudes. (Lombardozzi et al., 2018) illustrates the CO_2 and climate impacts. The total ecosystem carbon changes by gaining carbon via CO_2 fertilization effect and losing carbon by climate

change impacts Net Primary Production. The increase in CO_2 are supposed to warm climate (Meehl & Tebaldi, 2004) and increase precipitation (Wigley & Jones, 1985). The warmer climate increases atmospheric water holding capacity i.e. plant transpiration and soil water evaporation (Held & Soden, 2006) resulting in higher plant water demand (Lombardozzi et al., 2018) and hence reducing the water availability on land (Dai, 2011). In dry regions, vegetation greenness increased by 5 to 10 % with a concurrent increase of atmospheric CO_2 by 14%, globally (Donohue et al., 2013). CO_2 fertilization effects on vegetation and water availability in humid regions are yet to quantified.

The Southeastern United States is a wet region. The "wet regions get wetter" paradigm applies to the Southeastern US (Held & Soden, 2006; Kumar et al., 2013). The Southeastern US experienced water shortages during 2005-2007, which were associated with population growth (Seager et al., 2009). An extensive agricultural expansion was observed in the Southeast US from the late 19th century early 20th century, resulting in anthropogenic land-use change (Trimble, 2008; Wear & Greis, 2002). Then the forest industry gained popularity in the early 20th century followed by urbanization, which led to a decrease in forested areas in the Southeast US (Wear & Greis, 2002). The Southeastern US has undergone the highest rates of land-use and land cover changes from 1973-2011, nationally (Napton et al., 2010).

A long-term study is needed to quantify vegetation and climate change impacts on water availability in Southeast US. The forests generally take 30 years to reach maturity (Scott & Prinsloo, 2009). After reaching maturity, the transpiration, leaf area index, and interception stop increasing in the forest plants (Nagy et al., 2011; Scott & Prinsloo, 2009). Similarly, land-use change takes several decades to have a quantifiable signature at the regional scale (Kumar, Merwade, Rao, & Pijanowski, 2013).

1.2 Objectives

The overarching goal of this study is to quantify the impacts of land-use change and climate change on water resources at the regional (Southeastern US) scale. I use an interdisciplinary approach by combining hydrology and climate science. Long-term hydrological observations help to understand the historical change in the region and climate models help to test the hypotheses about the observed changes by performing a single-factor analysis experiments. The study focuses on the following objectives:

1. **Assess the observed hydrological and vegetation changes in the Southeastern United States using streamflow and NDVI observations**

   The water dynamics are critically changing due to the increasing population and irrigation in the Southeast US. Further, climate change and vegetation change can affect water availability. Hence, the first objective of my study is to assess long-term climate, vegetation, and hydrological changes in the Southeast US. I use observed streamflow data for water availability, Parameter-elevation Regressions on Independent Slopes Model (PRISM) precipitation and temperature data for climate trends, and satellite observations for vegetation trend analysis.

2. **Quantify the role of climate change, land-use change, and CO_2 physiological response on water availability in the present and future climate.**

   Observed hydrological changes represent a combined response of climate change, land-use change, and CO_2 physiological and fertilization effects. I use the Community Land Model version 5 (CLM5) to isolate the effect of individual drivers. Community Land Model (CLM5) is a widely use land surface model that simulates regional and global scale

biogeophysical and biogeochemical processes (Lawrence et al., 2019). The model helps to understand the impact of vegetation changes, either natural or anthropogenic, on water and energy balance at the land surface. It considers the physical, chemical, and biological processes related to global environmental change. I will use a single factor experiment to isolate the role of climate change, land-use change, irrigation effects, and CO_2 physiological effects.

3. **Explain the observed water availability change as the complex interplay between climate changes, land-use change, and vegetation effect in the Southeast.**

   Finally, I will assess the relative contribution of each driver. I will conduct regional average analysis as well as spatially distributed analysis of the effect of individual drivers.

1.3 Organization of the Thesis

This thesis is organized as follows: Chapters 2 and 3 describe the major topics of this thesis in a self-contained manner, i.e., each chapter has an introduction, data and methods, results, discussions, and conclusion sections. A summary of findings is also presented at the end of each chapter. A synthesis is presented in Chapter 4.

Chapter 2. Budyko Analysis of Vegetation Effects in the SE USA

2.1 Introduction

Climate and vegetation play important roles in the water cycle (Wei et al., 2018), and understanding these help water resource managers to develop sustainable management strategies (Sun et al., 2017). Changes in the vegetation and climate can increase or decrease water availability (Liu et al., 2019; Qi et al., 2019; Wei et al., 2018; Wolf et al., 2018). For example, Trancoso et al. (2017) reported that vegetation and climatic changes reduce baseflow due to increasing atmospheric CO_2. Increased water use efficiency due to enhanced atmospheric CO_2 increases photosynthetic activity reduces baseflow. Vegetation and climate equally contribute to changes in available water (Li et al., 2017), affecting groundwater, vegetation growth, and feedbacks (Liu et al., 2019b). Vegetation impacts the groundwater-streamflow connection (Kinal & Stoneman, 2012) and also groundwater recharging rate (Dawes et al., 2012). Increased plant growth and warming, increases bulk plant water demand resulting in the reduced runoff, despite increased total water use efficiency (Buermann et al., 2018; Mankin et al., 2019). The Budyko framework, which is a heuristic approach to conceptually partition precipitation into evapotranspiration and streamflow using just a few model parameters (Budyko, 1958; Fu, 1981; Kumar et al., 2016; L. Zhang et al., 2008). The Budyko framework has been tested, validated, and applied in numerous observational and modeling-based studies, and remains an active research area to understand land-atmosphere interactions (Koster & Suarez, 1999; Kumar et al., 2016; Padrón et al., 2017; Roderick & Farquhar, 2011; D. Yang et al., 2009; L. Zhang et al., 2008). It comprises of two independent variables: Dryness Index and catchment efficiency parameter *"w"* (Kumar et al., 2016). Dryness index is the ratio of potential evapotranspiration to

Precipitation. The Budyko framework provides a data-driven holistic approach to understand climate and vegetation effects on water availability (Donohue, Roderick, & McVicar, 2012).

This study aims at understanding the long-term impacts of climate and vegetation on water resources in the Southeastern United States, a humid region with significant forest cover, and to assess the role of vegetation and climate as the dominant drivers of streamflow change using the Budyko framework. Determining how vegetation cover and climate changes affect hydrology in watersheds can advance our understanding of water cycle projections in the region.

2.2 Data and Methods

2.2.1 Data:

The long-term (1951 to 2015) streamflow data from the United States Geological Survey (USGS) was utilized (Figure 6). Geospatial Attributes of Gages for Evaluating Streamflow (GAGES-II) (Falcone et al., 2011) was used for selecting reference stations that have minimal human interferences. Based on the GAGES-II database, I have selected 47 watersheds that are in near-natural conditions and have continuous data available.

For each watershed, I downloaded monthly 4-km spatial resolution data from 1950 to present from the PRISM-Climate Group (Parameter-elevation Regressions on Independent Slopes Model). In particular, datasets include precipitation, temperature (daily minimum, t_{min}; and daily maximum, t_{max}). The average temperature was computed from minimum and maximum temperature (Daly et al., 2008; Daly et al., 1994). CRUNCEP data is used for calculating potential evapotranspiration. CRUNCEP is combination of two datasets for 110-year (1901-2010) dataset (Viovy, 2011):

1. CRU TS3.2 is monthly half grid data for 1901-2002 time period (Mitchell & Jones, 2005).
2. NCEP Reanalysis is 6-hourly data with spatial resolution of 2.5 degree for 1948 to 2010.

Normalized Difference Vegetation Index (NDVI) is a standardized index for greenness. It is computed as: $NDVI = \frac{NIR-VIS}{NIR+VIS}$, where NIR and VIS stands for pixels from near-infrared radiation and visible or red radiation, ranging between -0.2 and 1.0, from bare lands or no vegetation to dense vegetation. NDVI from AVHRR (Advanced Very High-Resolution Radiometer) has very high resolution (0.05 degrees) data ranging from July 1981 to December 2015 (Vermote et al., 2014).

2.2.2 Methodology:

Water balance: Equation 1 describes the water flows into and out of the hydrological system as follows:

$$\Delta S_w = P - ET - R \qquad (1)$$

where ΔS_w, is water storage change (surface and soil), P is precipitation, ET is evapotranspiration, and R is runoff, including rechange to the groundwater, respectively.

Over the decadal time scale, the water storage (ΔS_w) from equation (1) is zero if no deep recharge is assumed (Bonan, 2016). Therefore, all the precipitation (P) falling on the ground is either lost as runoff (R) or evapotranspiration (ET). The factors affecting the rate of evapotranspiration at a longer time scale in Budyko hypothesis are available energy and water. For given atmospheric and radiative conditions, Potential evapotranspiration (PET) is the surface evapotranspiration (ET) rate that would hold if the soil and vegetation were well watered

(Scheff & Frierson, 2014). Evapotranspiration (ET) is the quantity of water that is actually removed from a surface due to the processes of evaporation and transpiration. Potential evapotranspiration (PET) and precipitation (P) represents two limits: available energy and available water limits, respectively.

The Budyko model is a function of Dryness Index (DI) and a catchment efficiency parameter (w). Dryness Index is the ratio of potential evapotranspiration to the precipitation ($\mathrm{DI} = \frac{\mathrm{PET}}{\mathrm{P}}$). The Budyko model is given in equation 2 (Fu, 1981):

$$\frac{ET}{P} = 1 + \frac{PET}{P} - \left[1 + \left(\frac{PET}{P}\right)^{w}\right]^{\frac{1}{w}} \quad (2)$$

Here the parameter "*w*" is a catchment efficiency parameter ranging from 1 to ∞. A higher "*w*" represents a greater efficiency of the catchment for converting precipitation into evapotranspiration (Zhang et al., 2008). In other words, more is the "*w*" more are the transpiration losses from land, or higher is the atmospheric water addition.

Runoff ratio is the ratio of runoff or streamflow to the precipitation ($\mathrm{RR} = \frac{\mathrm{R}}{\mathrm{P}}$). For runoff ratio (RR) analysis (Eq. 3), the Budyko equation (Eq. 2) can be combined with the water balance equation (Eq. 1) assuming the long term storage change to be negligible (Zhang et al., 2008).

$$RR = \frac{\mathrm{R}}{\mathrm{P}} = -\mathrm{DI} + (1 + \mathrm{DI}^{\mathrm{w}})^{\frac{1}{\mathrm{w}}} \quad (3)$$

Li et al. (2013) has derived the following relationship relating w and NDVI to incorporate the vegetation effects to the Budyko model:

$$\mathrm{w} = 2.36 * \left(\frac{\mathrm{NDVI} - \mathrm{NDVI}_{min}}{\mathrm{NDVI}_{max} - \mathrm{NDVI}_{min}}\right) + 1.16 \quad (4)$$

Inter-annual variations in runoff are quantified with the assumption that inter-annual variations in water storage change are small (Koster & Suarez, 1999). Therefore, *runoff deviation ratio* is the ratio of the standard deviation of annual streamflow (runoff, σQ) to the standard deviation of annual precipitation (σP; Zhang et al., 2008):

$$\frac{\sigma Q}{\sigma P} = (\mathrm{DI}^{w} + 1)^{\frac{1}{w}} - DI + DI\left(1 - DI^{w-1}(DI^{w} + 1)^{\frac{1}{w}-1}\right) \quad (5)$$

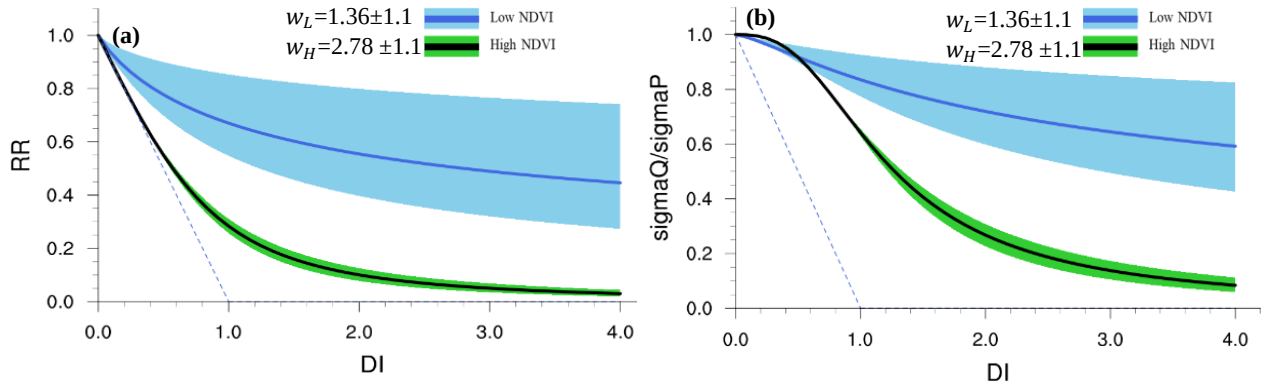

Figure 1. (a) Runoff ratio and (b) runoff deviation ratio from the theoretical understanding. Units (NA)

From the previous theoretical understanding, equations 3 and 5 are formulated for runoff ratio (Figure 1a) and runoff deviation ratio (Figure 1b). Figure (1) shows that with larger vegetation NDVI (green line), there are larger decreases in the water availability. Also, the 95% confidence interval is computed for both low ($W_L = 1.36 \pm 1.1$) and high ($W_H = 2.78 \pm 1.1$) vegetation scenarios. Increasing *"w"* value shows that uncertainty decreases. In other words, Figure 1 shows that with increase in control value of "*w*", there is decrease in the uncertainty for runoff ratio and interannual variation of runoff ratio. Since "*w*" is catchment vegetation characteristic parameter (equation 4), therefore with an increase in the "*w*", runoff ratio will be reduced significantly because more water will leave the watershed through ET.

Wet (dry) regions are defined as those when potential evapotranspiration is less (more) than precipitation (Kumar et al., 2016). Classification of regions as humid, transition and dry is based on the dryness index, i.e. DI < 1, 1 < DI < 2 and DI > 2, respectively. Dry regions are the water-limited regions, and humid regions are energy limited.

2.2.3 Cluster Analysis for forty-seven watersheds in the Southeast US: The southeast United States is a humid region mainly comprising of dryness index less than one (Figure 2a). Selected watersheds in this region are further classified as low and high vegetation density, using a cluster analysis for NDVI data (Figure 2b). The average NDVI value was 0.65, and low vegetation density areas from the cluster analysis were always lower than the average NDVI value. There were 22 low vegetation density watersheds in the Southeast US and 25 high vegetation density watersheds. The black boundaries in Figure (2a) and (2b) outline the forty-seven watersheds selected based on availability of continuous daily data record, along with more than 1000 square km area and are natural watersheds (Falcone et al., 2011).

2.2.4 Budyko Analysis using observed streamflow, NDVI, and precipitation data: I have analyzed the runoff ratio and runoff deviation ratio for 47 watersheds across the United States. To compute RR, I averaged the streamflow data from 1981 to 2010 and computed annual

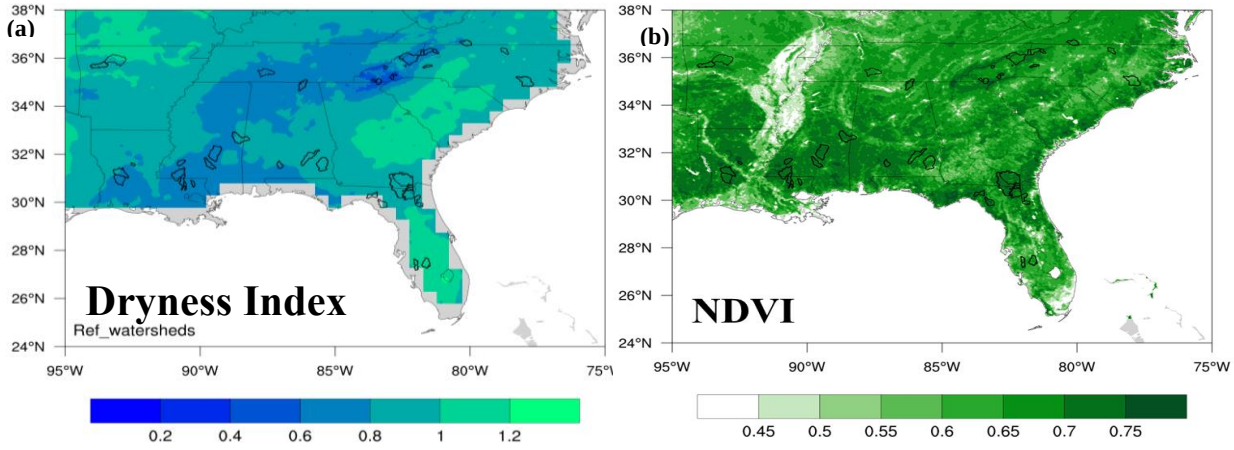

Figure 2. (a) Dryness Index and (b) NDVI for watersheds in Southeast United States. Units (NA)

average streamflow for each watershed. The area average precipitation for the corresponding period was computed using PRISM precipitation data. Then, I computed RR for each watershed by dividing observed streamflow with PRISM precipitation data.

The second step in the calculation was computing the catchment efficiency parameter "*w*" in the Budyko Model (equation 4), because on calculating "*w*" from NDVI gives average value of 0.65, which can be only used in large watersheds(Li et al., 2013) . Since this study constitutes small watersheds as well, therefore, "*w*" parameter is optimized. I estimated the parameter (w) by employing the nonlinear optimization function using DI as an independent variable and RR as a dependent variable and 'w' as a model parameter as given in equation 3 (Kumar et al., 2016). The parameter '*w'* is estimated locally using the 30-year climatology of RR and DI, using all available observed data. We performed nonlinear optimization using equation 3 and given values of RR and DI from the observations. We used the optimized w for runoff deviation ratio using $\frac{\sigma Q}{\sigma P}$ and DI from observed data and equation (5).

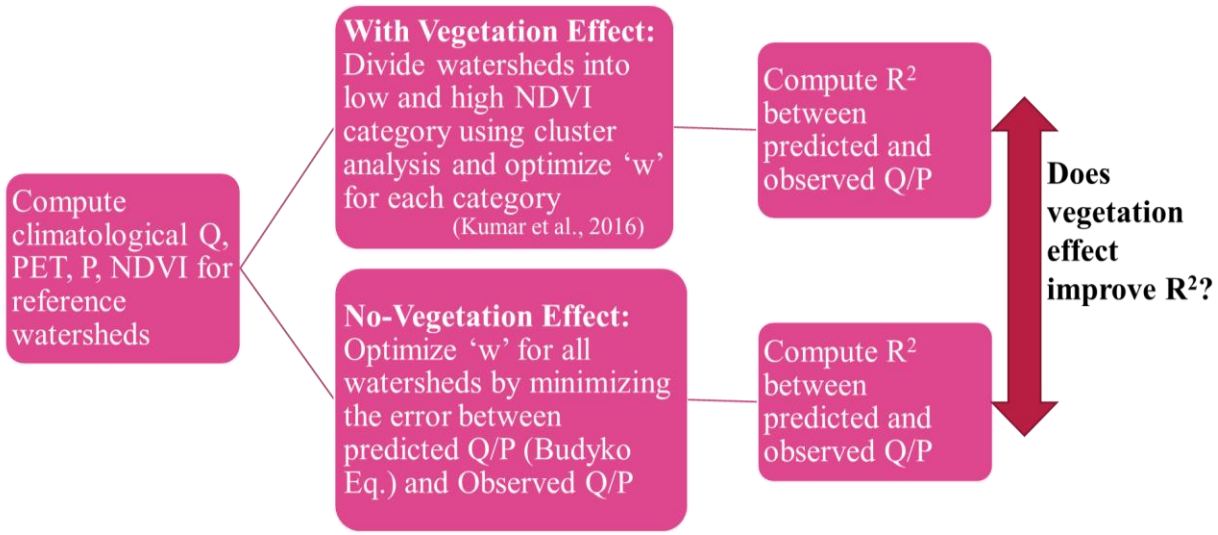

Figure 3. Application of Budyko Framework to investigate vegetation effects

2.2.5 Hypothesis testing for vegetation effects using Budyko model and observed data

Figure 3 explains the methodology for hypothesis testing. Assuming that vegetation does not impact the water availability, the catchment parameter *"w"* was optimized as described above and then statistical analysis was conducted and "R^2" was computed. Similarly, to account for the "vegetation effects" on the runoff ratio, we divided these watersheds into two categories, high and low NDVI (as discussed earlier) using cluster analysis followed by optimization of "*w*" parameter for both the categories, namely high and low vegetation. Then, R-square between the predicted and observed runoff ratio was computed between the observed RR and predicted RR for all 47 watersheds. In other words, the latter analysis helped us to clarify that vegetation impacts the water availability.

2.3 Results and Discussion

In this humid region, the results demonstrate the negative impact of vegetation on the water availability. The R-square increases between the simulated runoff (Eq. 3) and the observation increased from 0.60 to 0.62 upon the incorporation of vegetation factor (Figure 4).

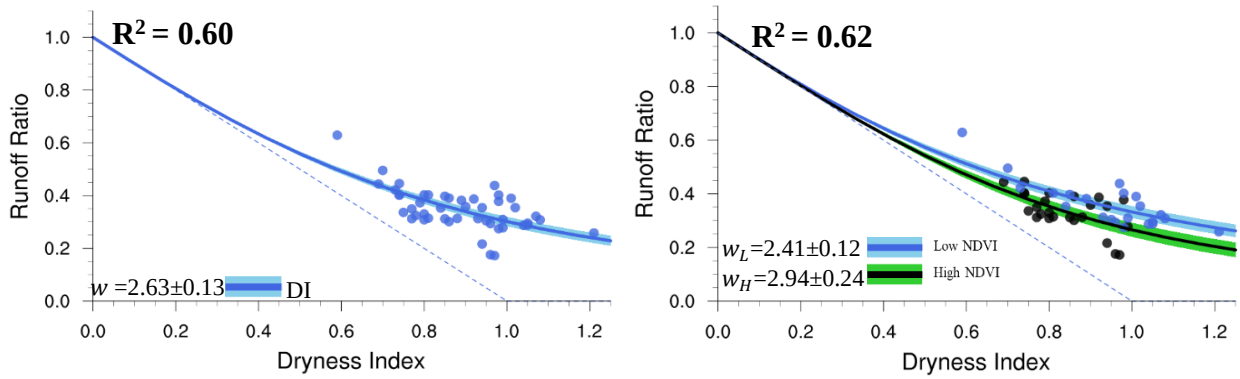

Figure 4. Runoff ratio with respect to (a) dryness index and (b) dryness index and vegetation for watersheds in southeast United States.

However, no change in R-square for the runoff deviation ratio is observed (Figure 5). The variability in runoff ratio is not impacted by the vegetation classification.

A minimal or no vegetation effects in runoff ratio variability can be due to the location and characteristics of watersheds. The watersheds are in humid region and all are forested, because I selected only reference watersheds that have minimal human interference, e.g. land-use change, and urbanization. These forested watersheds can result in minimum variability in vegetation. Also, the sample size for this study is not large enough, therefore vegetation might not impact the interannual variability in the runoff ratio. Another contributor to water availability changes can be the climate. The runoff variability show significant correlation with climate variability is El Nino Southern Oscillation (ENSO) (Newman et al., 2016). It is likely that vegetation plays a secondary role for the runoff variability.

Other climatic drivers can include changes in radiation, temperature and wind (e.g., Penman-Monteith equation (Monteith, 1965; Penman, 1948)). Catchment *"w"* can also change with climate change due to increasing CO_2 effects (Kumar et al., 2016). A warming climate can increase evapotranspiration losses and reduce the available water. Temperature analysis using

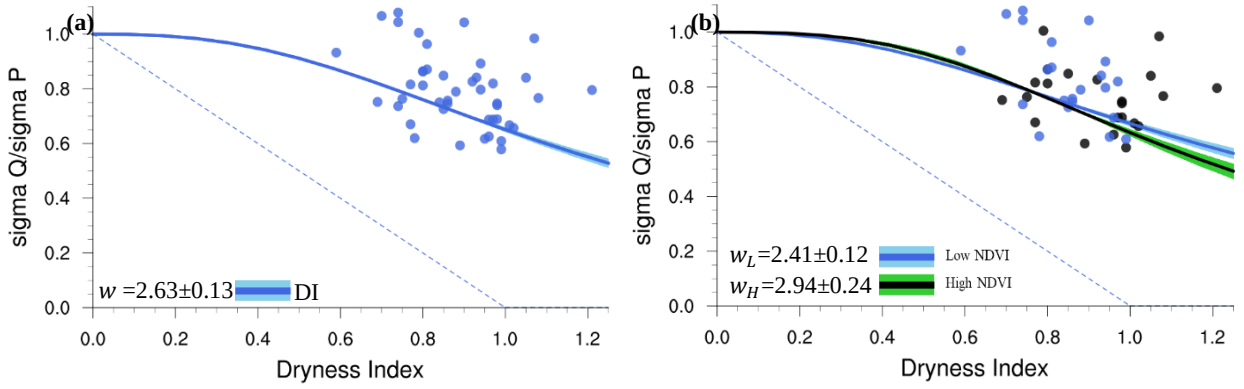

Figure 5. Runoff deviation ratio with respect to (a) dryness index and (b) dryness index and vegetation for watersheds in southeast United States. Units (NA)

GISS data show no significant warming in the Southeastern United States (Figure A2). The increase in CO_2 will have two major vegetation responses affecting *"w"*:

1. Water Use Efficiency (WUE): WUE is the ratio of water loss to carbon gain. WUE increases due to a reduction in stomatal opening under elevated CO_2 concentration resulting in increased water availability (Medlyn et al., 2011).
2. Plant Growth: decreases water availability due to higher photosynthesis rate under elevated CO_2 concentration (Gray et al., 2016).

Exploratory Analysis: Finally, I conducted a cross-correlation analysis (Table 1) among all the available variables to determine their relative influence on total water availability. I found that the dryness index significantly negatively correlates to the runoff ratio (-0.60). Potential evapotranspiration is also negatively correlated with the runoff ratio (-0.58). The increase in the evapotranspiration losses due to an increase in transpiration by CO_2 increase can result in decrease of streamflow or available water.

Table 1. Correlation analysis for water-related variables in humid watersheds

Correlation (47 watersheds)						
	RR	DI	NDVI	PCP	PET	Streamflow
RR	1	-0.60*	0.04	0.17	-0.58*	0.86*
DI		1	-0.64*	-0.75*	0.21	-0.84*
NDVI			1	0.78*	0.38*	0.41*
PCP				1	0.46*	0.63*
PET					1	-0.21
Streamflow						1

*p = 0.05 (significant at 5% level of significance)

Vegetation does not show a significant impact on runoff ratio using linear analysis, i.e. NDVI and RR correlation is 0.04. Vegetation impact is important in the context that hydrologic fluxes show a nonlinear relationship with climate and vegetation inputs (Zhang et al., 2008). Hence, a nonlinear Budyko model helps to disentangle the effects of vegetation on streamflow (Kumar et al., 2016). Budyko model shows that incorporating vegetation effects improve water availability predictions. Also, the streamflow positively correlates with the runoff ratio (0.86), indicating that RR is a good predictor of total water availability.

The dryness index is negatively correlated to vegetation (-0.64), and precipitation (-0.75). Since precipitation and dryness are inversely related in Eq. 3. In Table 1, vegetation is positively correlated with the precipitation (0.78), followed by streamflow (0.41) and PET (0.38). Therefore, precipitation is a significant determinant of spatial variability in vegetation in this region. Climate comes out to be first order driver and vegetation as second order driver. In summary, climate variability derives the vegetation (Padrón et al., 2017) and which act to modulate the response as runoff ratio further.

2.4 Conclusions

The southeastern US is a humid region. Vegetation plays an important role for analyzing water availability in this region. Vegetation negatively impacts the water availability in the region. More is the vegetation, higher is the photosynthetic rate increasing the NDVI resulting in enhancement of transpiration losses and hence, decrease in water availability. The results indicated that the incorporation of vegetation effects in the Budyko model improved the R-square from 0.60 to 0.62. No or minimal impact of vegetation on the interannual variation of

runoff ratio variability was observed, that can be due to selection of watersheds in forested region, resulting in low variation in vegetation.

Chapter 3. Climate Modeling Experiments

3.1 Introduction

There are significant uncertainties in water cycle projections at regional scales (Cook et al., 2018; Greve et al., 2014; Kumar et al., 2015; Kumar et al., 2013). Sources of uncertainty include changes in atmospheric circulation, representation of coupled carbon-water-energy cycles and their parameterizations in climate models, land-use change, and water management (Allan, 2014; Bonan, 2016; Chang et al., 2015; Langenbrunner et al., 2015; Lehner et al., 2019). A process-oriented approach helps quantify relative contributions to different sources. We quantify relative contributions on water availability change in the Southeastern United States (SE US) from five potential drivers: climate change, land-use change, irrigation, increased water use efficiency, and plant growth under elevated CO_2 concentration.

The roles of climate change and land-use change have been thoroughly investigated in climate and hydrology literature. Current projections suggest that climate change will lead to increased heavy precipitation in the SE US, therefore increased risk of flooding (Held & Soden, 2006; Kumar et al., 2015; Wuebbles et al., 2017). Additionally, forest to agriculture conversion and urbanization increase water availability due to less evapotranspiration (Bonan, 2016; Bormann & Likens, 2012; Schilling, 2016; Swank et al., 1988). Warmer temperatures can increase evapotranspiration, therefore decrease water availability (Cook et al., 2018; Dai, 2013).

As CO_2 increases, plants respond with: (1) increased water use efficiency (WUE) due to reduction in stomatal opening under elevated CO_2 concentration (Medlyn et al., 2011), and (2) increased plant growth, also known as the CO_2 fertilization effect, due to higher photosynthesis rate under elevated CO_2 concentration (Gray et al., 2016). Recent studies have suggested that the WUE effect can ameliorate the effects of increasing dryness associated with climate change in

some regions (Fowler et al., 2019; Lemordant et al., 2018; Swann et al., 2016; Yang et al., 2019). However, increased plant growth leads to more leaves, which can increase whole-plant transpiration despite the lower leaf-level stomatal conductances. For example, a metanalysis of CO_2 enrichment studies found a 32±4% increase in plant growth due to the doubling of atmospheric CO_2 concentration (Wullschleger et al., 1995). (Frank et al., 2015) found increased transpiration despite decreased stomatal opening in the European forest and hypothesized that the combination of increased evaporative demand and plant growth could be responsible for the increased transpiration. Based on climate model projections, Mankin et al. (2019) found that plant growth could negate the effects of increased WUE on runoff in the warming climate scenarios. However, consistent comparison of different drivers of hydrological changes at the regional scale and their verification using observations need further investigations.

Observed streamflow changes reflect the integrated response of climate change, vegetation and land-use change, and direct human intervention in the hydrologic system. The United States Geological Survey (USGS) provides long-term streamflow observations from approximately 10,000 stations, several of which have continuous records since the 1950s (Eberts et al., 2019; Falcone, 2010). During the same time, the atmospheric CO_2 concentration has risen steadily since the 1950s, from 316 ppm in 1959 to 408 ppm in 2018 (Tans & Keeling, 2019). The first objective of this study is to investigate changes in the observed water availability or streamflow in the SE US. For example, (Trancoso et al., 2017) investigated long-term streamflow observations from eastern Australia and found a reduction in the base flow and attributed this change to the increased vegetation activity under elevated CO_2 concentration in the atmosphere. (Ukkola et al., 2016) found a 24-28% reduction in observed streamflow due to plant growth in semi-humid and semi-arid catchments of Australia.

The second objective of this study to quantify relative contributions of five potential drivers: climate change, land-use change, irrigation, increased water use efficiency, and plant growth under elevated CO_2 concentration. The SE US is a humid region (Fig. 6a) with an annual average precipitation of 1350 mm/year, and hence plant growth is generally not limited by water stress. Forests occupy more than 60% of the land area in the region (Fig. 6b). Hence, we expect that plant response is playing a dominant role in water availability changes in the SE US. The region has not experienced significant warming during the 20th century, likely due to the influence of multi-decadal climate variability that is countering the greenhouse gas radiative forcing (Kumar, Kinter, et al., 2013; Meehl et al., 2015; Pan et al., 2013). Cropland has declined during the 20th century due to low biophysical suitability in the SE US (Kumar et al., 2013). Conversion of cropland and natural forest to the developed area and commercial forestry has been the primary land-use trend from 1973 to 2011 (Napton et al., 2010; Sayler et al., 2015; Sayler et al., 2016). The lower Mississippi River Valley is one of the most intensively developed irrigated agricultural regions in the United States (Massey et al., 2017). The irrigation has expanded due to frequent drought in the region (Alston, Babcock, & Pardey, 2010; McNider & Christy, 2007; Schaible & Aillery, 2012; Selman & Misra, 2016).

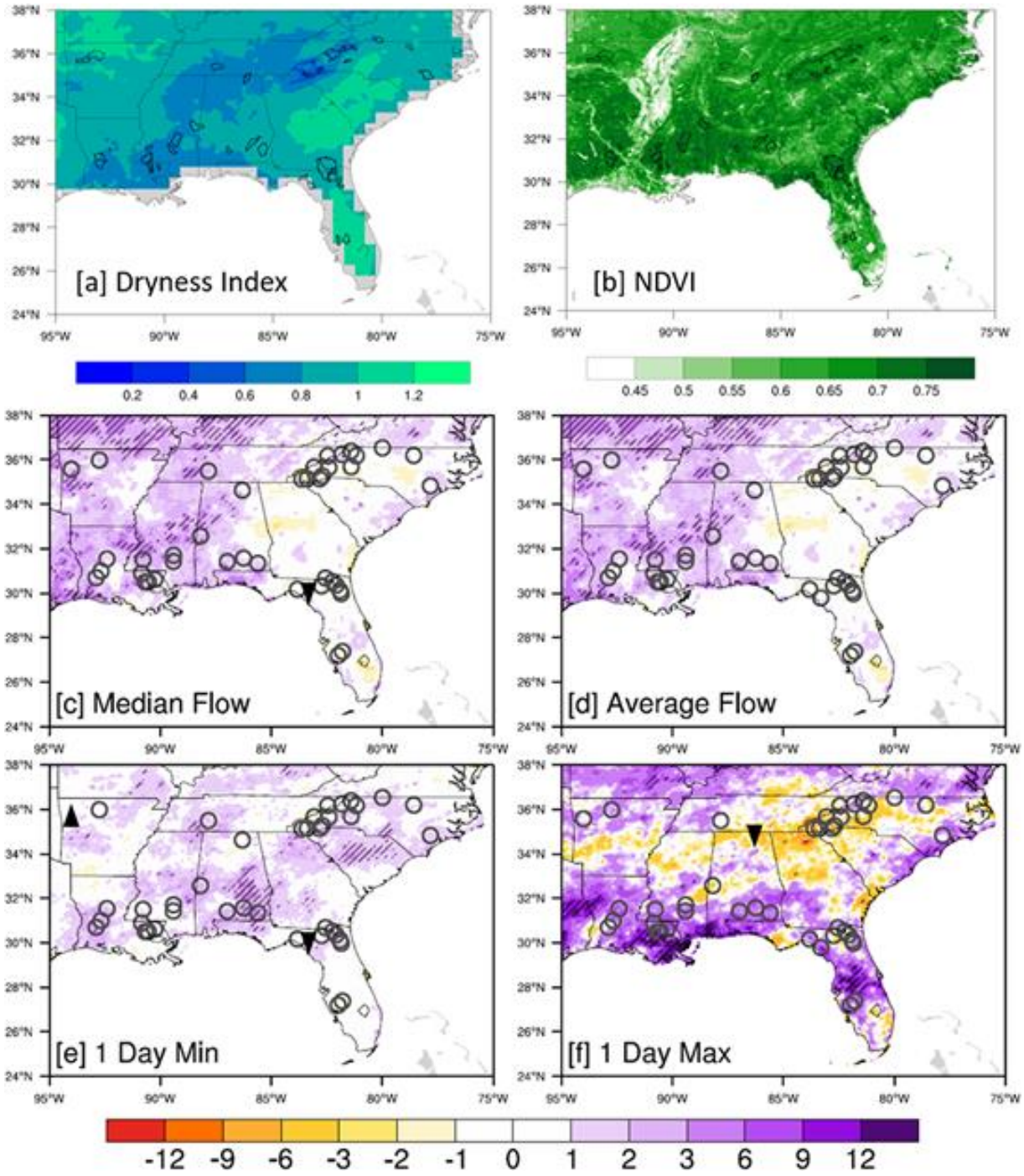

Figure 6. Streamflow and precipitation trends from 1951 to 2015 in the Southeastern United States**:** (a) dryness index and reference watersheds, (b) NDVI and reference watersheds, (c) – (f) streamflow trends are shown using circle (no trend), up arrows (increasing trends), down arrows (decreasing trend), and background color show corresponding precipitating trends from monthly

PRISM precipitation data. Dryness index is a ratio of climatological average potential evapotranspiration to precipitation, computed from 1981 to 2010 data as in (Kumar et al., 2016). The median and average flows are shown in the background of annual average precipitation trend, 1-day minimum flow is shown in the background of annual minimum monthly precipitation trend, and 1-day maximum flow is shown in the background of annual maximum precipitation trend. Hatching and up or down arrows indicate a statistically significant trend at the 95% confidence level. Trend significance is calculated using the non-parametric Mann-Kendall test with long-term persistence considerations. Unit: Dryness Index (NA), NDVI (NA), and Precipitation trend (mm per month per decade).

3.2 Data and Methods

3.2.1 Observations

We employ long-term USGS streamflow observations from 42 reference stations in the SE US that have minimal human interference and continuous daily records since the 1950s (Figure 6a and Table A1 of the Appendix) (Falcone et al., 2010). We analyze long-term trends in four streamflow statistics: annual median, annual average, annual 1-day minimum, and annual 1-day maximum flows to capture the full spectrum of the observed hydrological changes (Kumar et al., 2009).

Precipitation data from Parameter-elevation Regressions on Independent Slopes Model (PRISM) are used to assess the climate trends (Daly et al., 2008; Daly et al., 1994). PRISM uses climate observations from a wide range of monitoring networks, applies quality control measures, and topography dependent spatial interpolation techniques to develop high-resolution

(4-km) spatial climate datasets to reveal short-term and long-term climate patterns for the conterminous United States.

We use the normalized difference vegetation index (NDVI) and leaf area index (LAI) (Z. Zhu et al., 2013) to assess the long-term vegetation trend (1982 to 2010). The NDVI is a measure of vegetation growth that is remotely observed by the Advanced Very High-Resolution Radiometer (AVHRR) satellite (Vermote et al., 2014). The NDVI values range between –0.2 to +1; higher NDVI values indicate a greater photosynthetic rate by the plants (Myneni et al., 1997; Tucker et al., 1986) (Myneni et al., 1997; Tucker et al., 1986).

3.2.2 Nonparametric Trend Detection

We compute trends using the Theil-Sen method (Sen, 1968; Theil, 1992) (Eq. 2), and its significance is determined using nonparametric Mann-Kendall test (Kendall, 1975; Mann, 1945). If x_1, x_2, ……. ,x_n is a time series of given length n (in years), then magnitude of

$$TSA = median\left(\frac{x_j - x_i}{j - i}\right) \; for \; all \; i < j \qquad (1)$$

The trend significance calculation accounts for decadal to multidecadal climate variability or long-term persistence (LTP) in the time series and is described in (Kumar et al., 2009). The nonparametric method has the following advantages: (1) It contains no prior assumption about the linear trend, (2) it is more accurate in detecting trend (higher power) in nonnormally distributed data, for example, streamflow (Önöz & Bayazit, 2003; Yue et al., 2002), and (3) it is robust against outliers. The LTP presents a significant source of uncertainty that leads to an underestimation of variance in the time series and, therefore, can lead to a false identification of significant trends (Koutsoyiannis & Montanari, 2007). We determine LTP using the Hurst

coefficient (H) as the maximum likelihood estimator of a fractional Gaussian noise process. If H is statistically significant, then a modified variance is obtained (Hamed, 2008). This methodology successfully identifies multidecadal climate variability in the SE US (Kumar, Merwade, et al., 2013).

3.2.3 Single Factor Climate Modeling Experiments

We followed the Land Use Model Intercomparison Project (LUMIP) protocol (Lawrence et al., 2016) to isolate the role of climate, land use, irrigation, WUE, and plant growth changes on water availability in the SE US. We obtain the contribution of an individual factor by contrasting the control all-forcing experiment with a series of "one-factor-out" experiments (Table 2). We use the Community Land Model Version 5 (CLM5) (Lawrence et al., 2019) experiment because it has the most comprehensive dataset available for the analysis. Since the "Constant CO_2" experiment inhibits both WUE and plant growth effects, we performed additional "Stomatal Conductance Constant CO_2" experiment (described below) to separate the effects of WUE to that of the plant growth. The "Stomatal Conductance Constant CO_2" is a no WUE-only experiment. Hence, Control − Stomatal Conductance Constant CO_2 provides WUE-only effects, and Stomatal Conductance Constant CO_2 − Constant CO_2 provides plant growth-only effects. We also separated the effects of irrigation from that of land-use change (under rainfed agriculture) using CLM5 experiments (Table 2).

Additionally, we used the available Coupled Model Intercomparison Project Phase 6 (CMIP6) LUMIP data to assess uncertainties in CLM5 results (Eyring et al., 2016; Lawrence et al., 2016).

Table 2. List of CLM5 Experiments Used for Single-Factor Analysis

Factor	***Experiments***
Climate	Control [(a)] – Constant Climate [(b)]
Land-Use	No Irrigation[(c)] – No Land Use [(d)]
Irrigation	Control[(a)] – No Irrigation[(c)]
WUE (CO_2 Physiological)	Control[(a)] – Stomatal conductance constant CO_2[(e)]
Plant Growth (CO_2 fertilization)	Stomatal conductance constant CO_2[(e)] - Constant CO_2[(f)]
WUE & Plant Growth	Control[(a)] – Constant CO_2[(f)]
Land-use & irrigation	Control[(a)] – No Land Use[(d)]

Note: These experiments follow the LUMIP land-only experiment protocol as described by Lawrence et al. (2016).

[(a)] Control includes all factors with GSWP3 climate forcing.

[(b)] Constant climate — same as control but with pre-industrial climate forcing by looping over the first 20 years (1850 to 1869) of meteorological forcing data.

[(c)] No Irrigation—same as control with no irrigation.

[(d)] No Land-use—same as control with no land use.

[(e)] Stomatal Conductance Constant CO_2—same as control, but CO_2 concentration in stomatal conductance calculation is kept at the pre-industrial level (see text).

[(f)] Constant CO_2—same as control but CO_2 concentration in the atmosphere is kept at the pre-industrial level (285 ppm).

3.2.4 Model Description

The Community Land Model version 5 (www.cesm.ucar.edu/models/clm/) is an open-source (github.com/ESCOMP/ctsm) process-oriented community model. CLM5 simulates a range of biophysical and biogeochemical processes, including representation of land surface heterogeneity, canopy radiation, momentum, and energy balance, hydrology, photosynthesis, and stomatal conductance, carbon and nutrient cycling, land-cover and land-use change, crops, and crop management including irrigation and fertilization (Lawrence et al., 2019). CLM5 includes a prognostic annual cycle of vegetation evolution, emergence and senescence of leaves, and vegetation heights based on the Biome-biogeochemical cycle model (Thornton et al., 2002; Thornton & Rosenbloom, 2005). CLM5 calculates stomatal conductance using the Medlyn model (Equation 2) (Medlyn et al., 2011), which connects the water cycle (evapotranspiration) and carbon cycle (photosynthesis) in the model.

$$g_s = g_o + \frac{1.6\left(1 + \frac{g_1}{\sqrt{D}}\right) A_n}{\frac{C_s}{P_{atm}}} \qquad (2)$$

g_s refers to leaf stomatal conductance (μ mol m^{-2} s^{-1}), go stands for minimum stomatal conductance (μ mol m^{-2} s^{-1}), A_n is the leaf net photosynthesis (μ mol CO_2 m^{-2} s^{-1}), respectively. C_s refers to the CO_2 partial pressure at the leaf surface (Pa), and P_{atm} stands for atmospheric pressure (Pa). D is the vapor pressure deficit at the leaf surface (kPa) and g_1 represents a plant functional type-dependent parameter (μ mol m^{-2} s^{-1}). Keeping all other factors the same, increasing C_s will lead to a reduction in stomatal conductance and therefore increased WUE. We fixed C_s to its preindustrial level (28.55 Pa) in the "Stomatal Conductance Constant CO_2" experiment. Since we changed C_s directly in the conductance calculation while the atmospheric

CO_2 evolved as per the background state (default), the Stomatal Conductance Constant CO_2 experiment did not affect the carbon cycle in the model (shown later).

The photosynthesis rate increases with elevated CO2 concentration in the atmosphere (Dang et al., 1998). CLM5 uses the Farquhar et al. (1980) photosynthesis model for C3 plants and the Collatz et al. (1992) model for C4 plants as described by Bonan et al. (2011). An increased photosynthesis rate contributes to increased plant growth and higher LAI under elevated CO_2 concertation. Wieder et al. (2019) found that CLM5 response to the elevated CO_2 concentration is comparable with the observations from free air CO_2 enrichment (FACE) experiments (Ainsworth & Long, 2005).

3.3 Results

The streamflow observations show no significant trend from 1951 to 2015 (Figures 6c to 6f). Out of 42 reference stations, only one station shows a significant decreasing trend in median flow, two stations show a significant trend (one decreasing and one increasing) for 1-day minimum flow, and one station shows a significant decreasing trend in 1-day maximum flow. None of the 42 reference stations shows a significant trend for annual average flow (Figure 6c), which is the metric we use for further analysis.

Annual average precipitation shows an increasing trend in some areas, particularly towards the western part of the study region (Figure 6d). Heavy precipitation has generally increased towards the coast (Figure 6f), and trends shown here are consistent with other observational estimates (e.g., Kumar, Merwade, et al., 2013). Overall, despite increasing precipitation trends in parts of the SE US, the streamflow has not changed significantly.

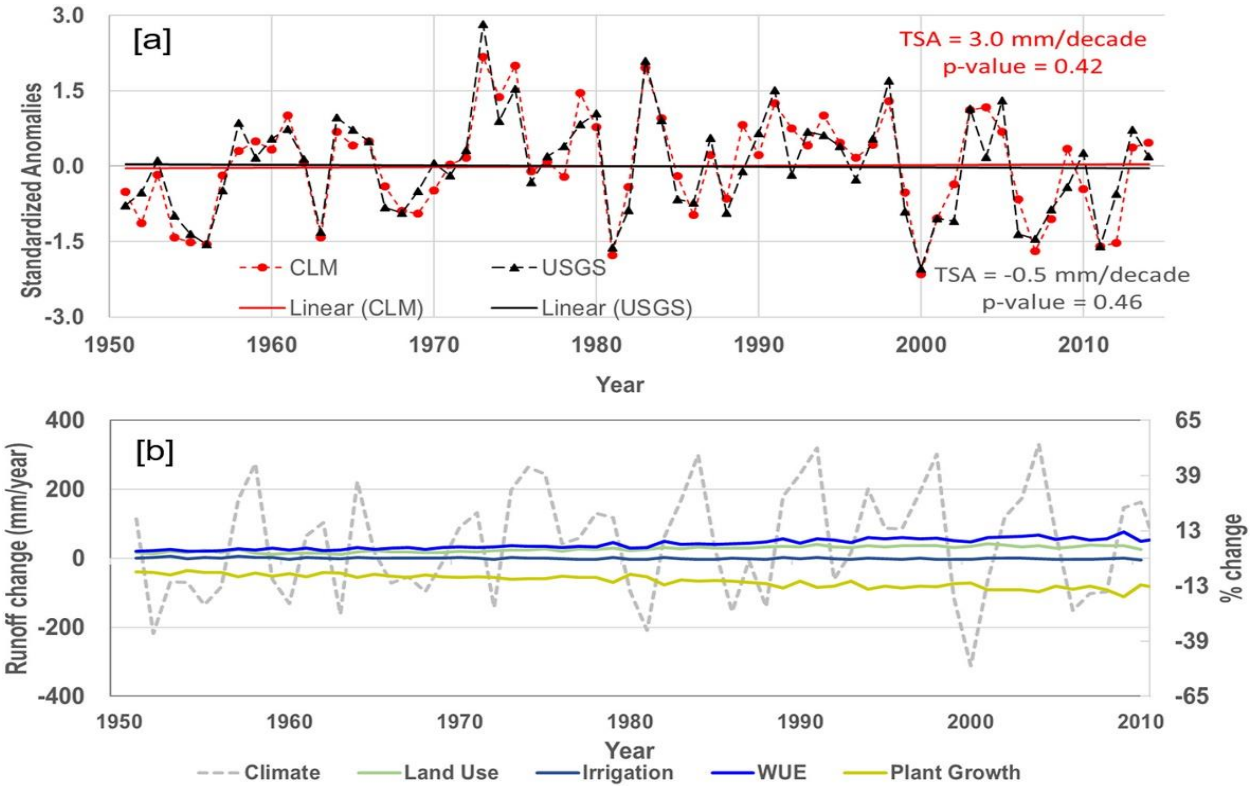

Figure 7. (a) Comparison CLM5 runoff in the control experiment with the USGS observations (area average for 42 reference stations). CLM5 results are computed from the area-weighted average of the grid-cells corresponding to the USGS watersheds. (b) contribution of drivers to the annual runoff change in CLM5 single factor climate modeling experiments, and the Southeastern US (24° north to 38° north, and 75° west to 95° west).

CLM5 captures the observed streamflow variability and changes in the Southeastern United States. Figure 6a compares average area streamflow from the 42 reference stations with the CLM5 control experiments. The CLM5 runoff data from the grid-cells corresponding to observations catchments (Figure 6a) are included in this analysis. We have used different terminologies: "streamflow" for USGS observations and "runoff" for climate model outputs mainly because of their prevalent use in the respective domain. We first computed area-weighted

average streamflow across 42 stations for each year from 1951 to 2015, and then we standardize the time series using its mean and standard deviation. The CLM5 and USGS observations compare well with a correlation value of 0.90. The CLM5, consistent with observations, does not show a statistically significant trend (p value <0.05) (Figure 7a). Similarly, the SE US regional average (24-38N, and 75-95W) CLM5 time series does not show a statistically significant trend (Figure 8). Hereafter, we have used the regional average time series for generality.

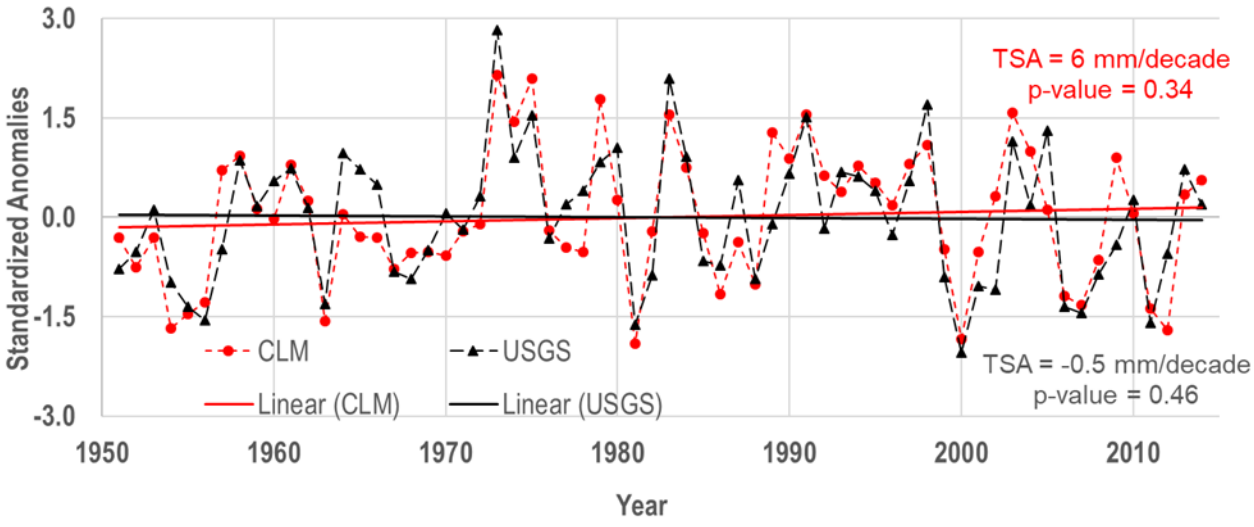

Figure 8. Comparison CLM5 runoff in the control experiment with the USGS observations (area average for 42 reference stations). CLM5 results are computed from the area-weighted average of the Southeastern US (24° north to 38° north, and 75° west to 95° west).

Plant growth is the most significant contributor that decreases runoff due to the increase in the LAI caused by the CO_2 fertilization effect. Figure 9 shows the average annual contributions from 1951 to 2010 due to each driver for runoff and LAI. Since climate impacts are highly variable (year to year), the mean climate impact is not statistically significant. Land-use

change and WUE increase runoff by 26.5 ± 2.0 mm/year and 42.4 ± 3.8 mm/year, respectively. Plant growth decreases runoff by 67.0 ± 4.9 mm/year due to a larger leaf area for total transpiration, which almost completely counteracts the combined effect of the land-use change and WUE. The changes in runoff stem from the corresponding opposite changes in evapotranspiration (Figure 10).

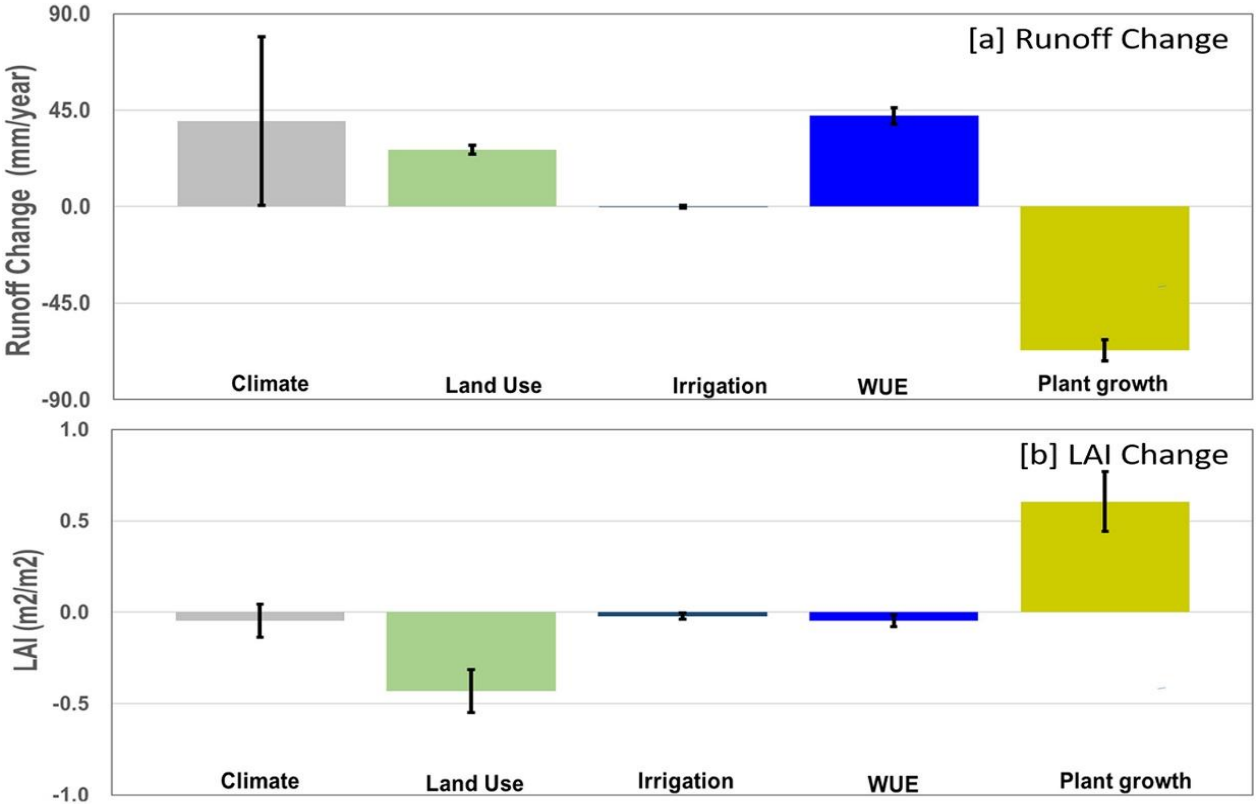

Figure 9. Contribution of individual drivers to (a) runoff change, and (b) LAI change. Annual average values from 1951 to 2010 for the Southeastern United States are shown. Error bars show two times the standard error estimate of annual mean values. If the error bar encompasses zero, then the mean change is not statistically significant (95% confidence level).

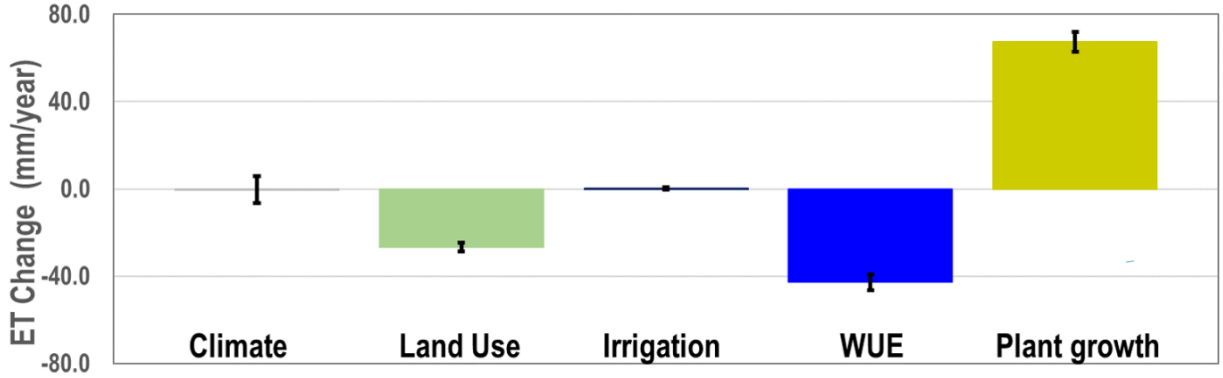

Figure 10. Contribution of individual drivers to evapotranspiration change. Annual average values from 1951 to 2010 for the Southeastern United States are shown. Error bars show two times the standard error estimate of annual mean values. If the error bar encompasses zero, then the mean change is not statistically significant (95% confidence level).

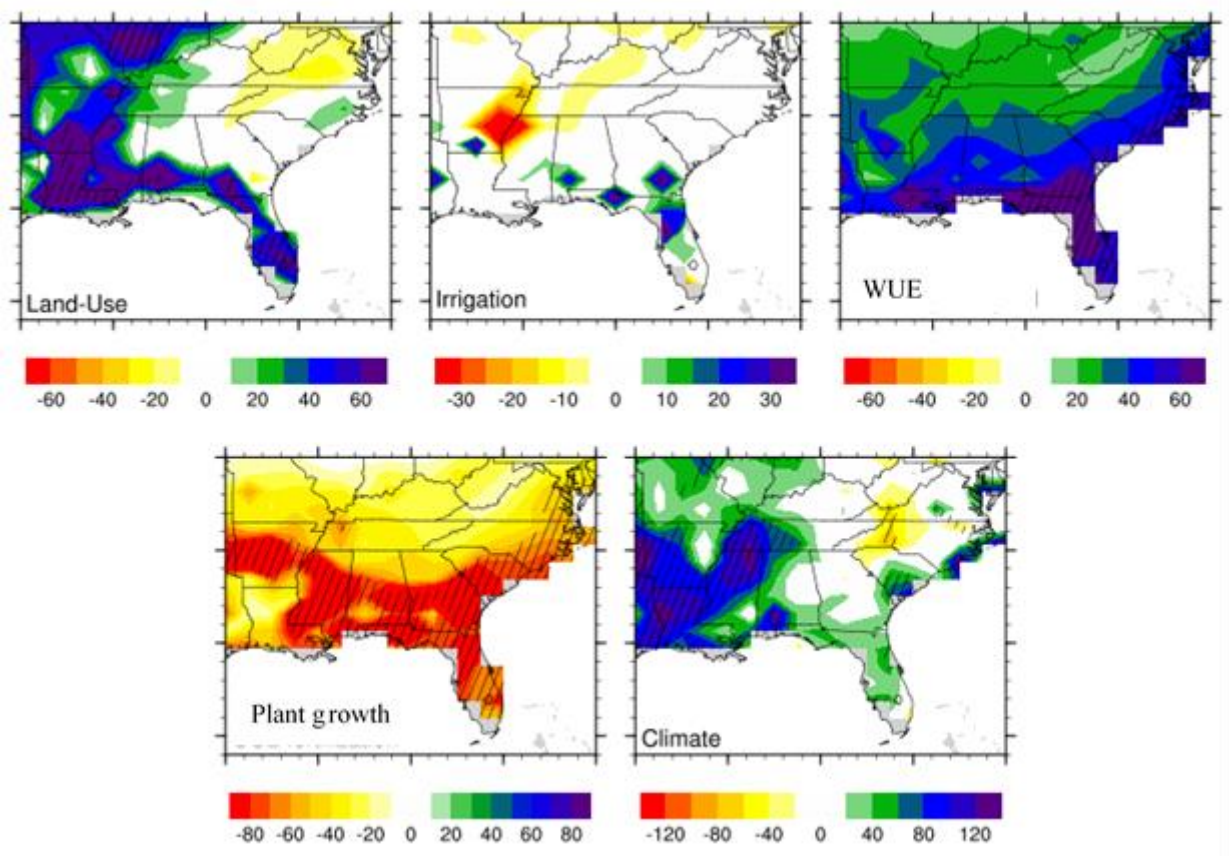

Figure 11. The spatial pattern of mean runoff changes (1951 to 2010) due to five drivers. Stippling show statistically significant change at the 95% confidence level based on the t-test. Unit: mm/year.

Figure 7b shows the contribution of the individual drivers on runoff change using CLM5 experiments (see Table 2). The climate impact is highly variable from year-to-year, attributable to the methodological design. The climate impacts are computed as the difference between control and constant-climate experiment, which recycles the preindustrial climate forcing (1850-1869) every 20 years (Table 2). This methodology of assessing climate impact is self-consistent with the methodology to determine the influence of other factors (Table 2). Land-use change and WUE both contributed to increases in runoff across the period 1951–2010. Plant growth, however, decreases runoff. Irrigation has minimal impact on the full region because of its relatively small areal coverage (Figure 11).

Higher CO_2 concentrations increase photosynthetic rates, increasing plant growth, and, therefore, LAIs. The simulated LAI change due to CO_2 fertilization is 0.61 ± 0.16 m2/m2. On the other hand, land-use change (mainly deforestation for urbanization and commercial forestry in this region) tends to decrease LAI (−0.43 ± 0.12 m2/m2). The contribution of other drivers to LAI change is not statistically significant. Note that our "Stomatal Conductance Constant CO_2" experiment did not exhibit statistically significant changes in LAI, as desired, thereby validating that this experiment design effectively separates the effects of WUE change from the effects of plant growth on runoff.

CLM5 response is qualitatively similar to the CMIP6 LUMIP multimodel mean response, although there are quantitative differences among models (Figure 12). For example, the

multimodel mean shows a net-zero combined effect due to WUE and plant growth, that is, the cancelation of the increasing water availability due to WUE by the plant growth. Similarly, all four CMIP6 LUMIP models show an increase in LAI due to elevated CO_2 concentration in the atmosphere. However, the CLM5 response of LAI change (0.56 ± 0.05 m2/m2) is greater than the multimodel mean change (0.33 ± 0.03 m2/m2) (e.g., Wieder et al., 2019). The CMIP6 LUMIP multimodel mean shows an increase in runoff due to land-use change and irrigation and high variability in climate effects similar to the CLM5 results.

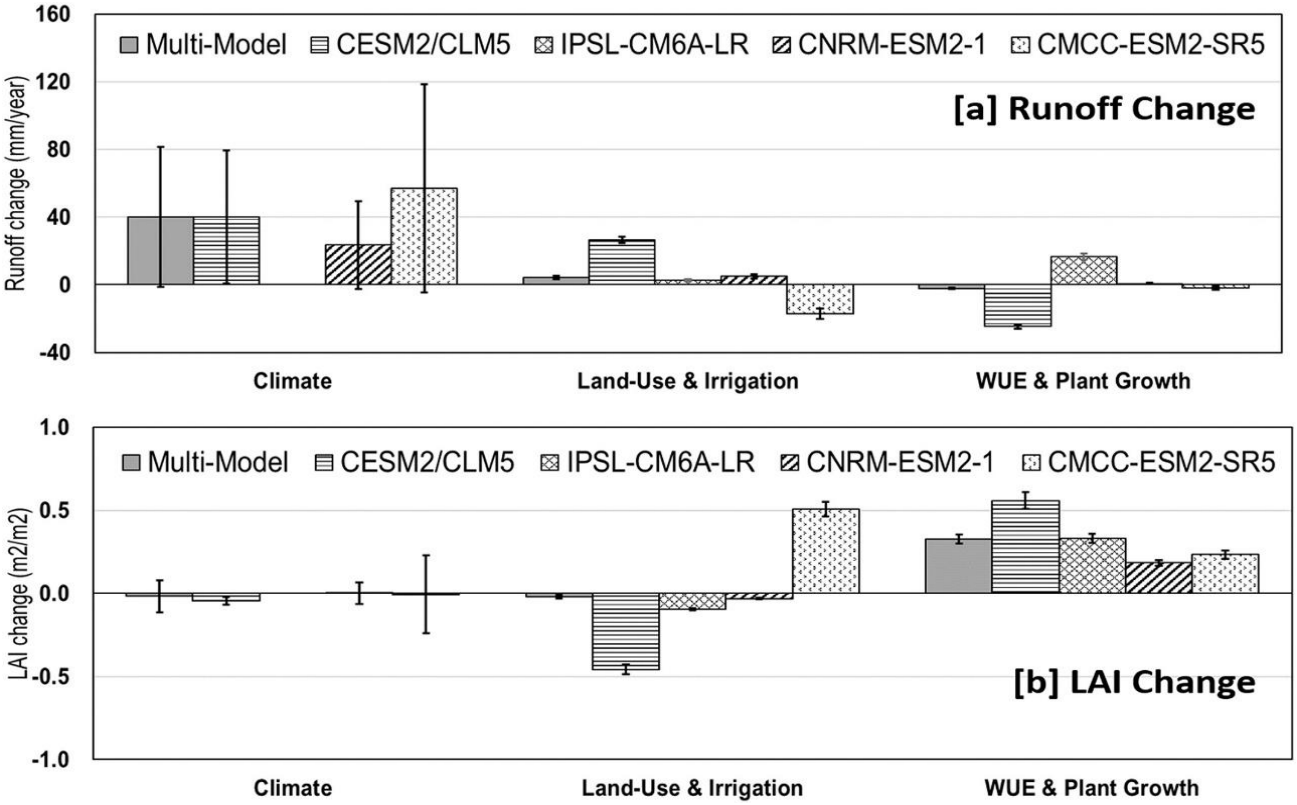

Figure 12. CMIP6 LUMIP multi-model mean and individual model results of the drivers of hydrologic changes in the Southeast United States for CMIP6 models. Only four CMIP6 LUMIP climate models and the combined effects of WUE and plant growth are investigated because of limited data availability (January 2020). Similarly, the combined effects of land-use change, and irrigation are investigated. IPSL-CM6A-LR model did not have a Constant Climate experiment.

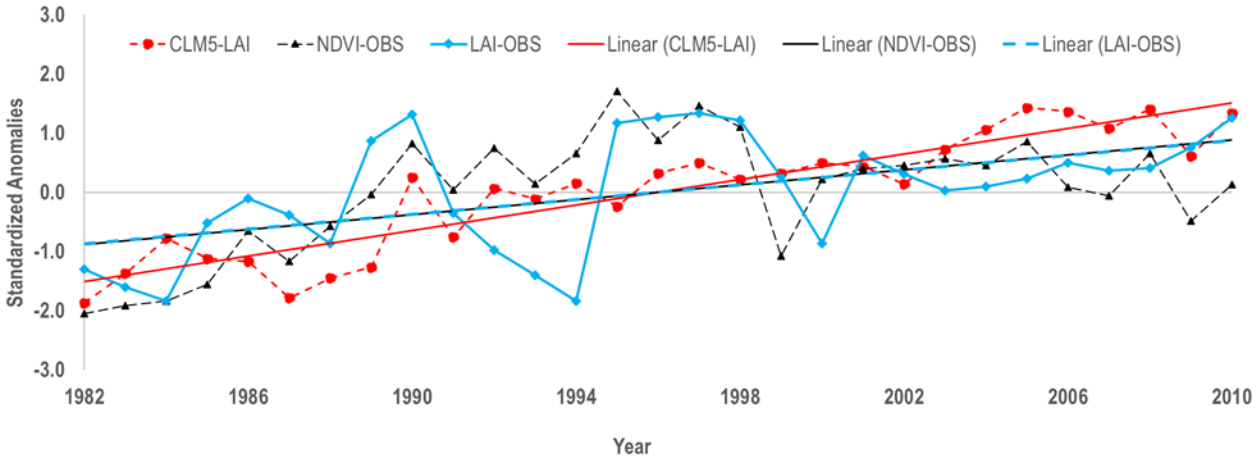

Figure 13. Standardized time series of NDVI and LAI from observations, and LAI from CLM5 control experiment and from the year 1982 to 2010 for the SE US. Respective trend estimates are: CLM-LAI: m^2/m^2 per decade (p-value < 0.05), AVHHR-LAI is 0.03 m^2/m^2 per decade (p-value = 0.11), and AVHHR-NDVI is 0.01 per decade (p-value = 0.18).

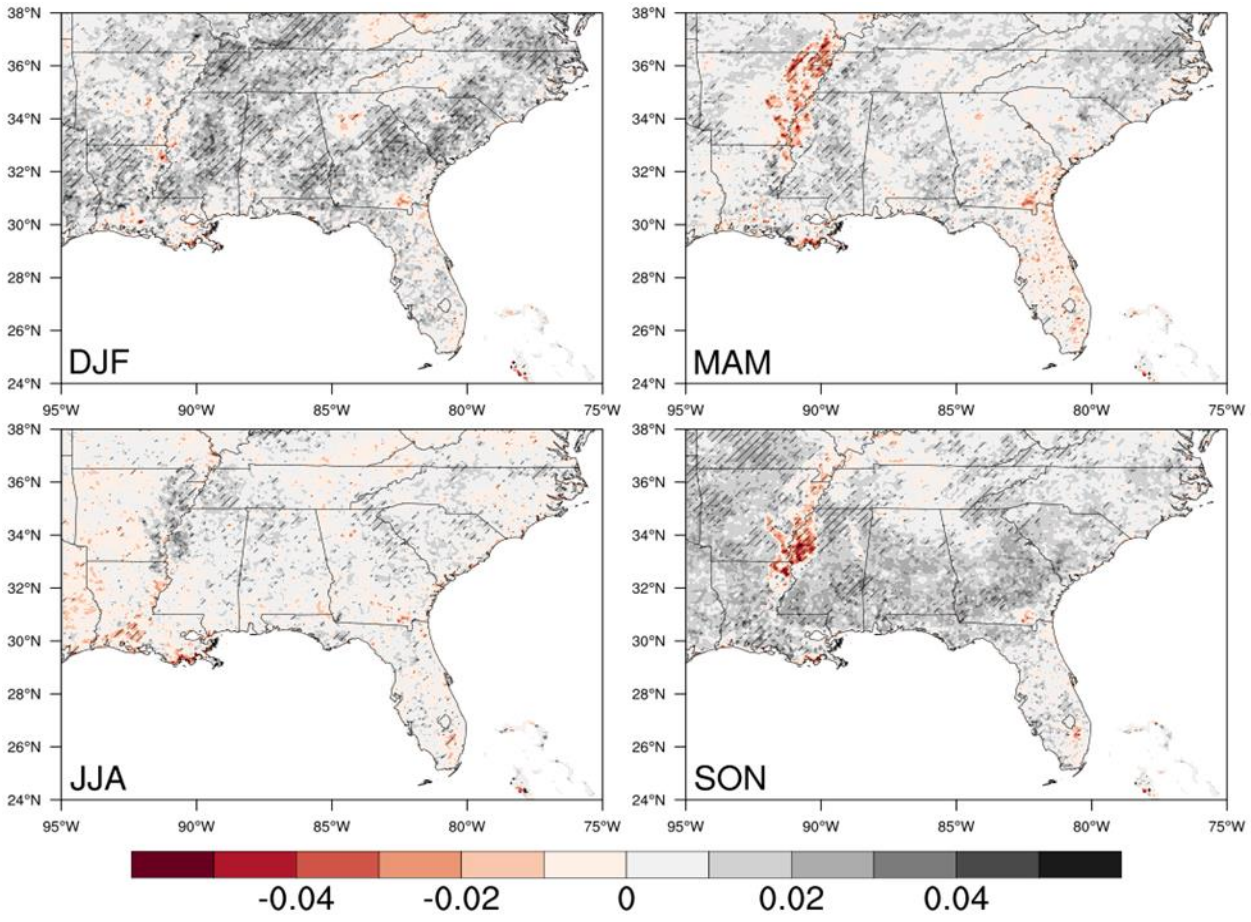

Figure 14. Trends in satellite observed NDVI from 1982 to 2015. Color contours show trend magnitude. Hatching denotes a statistically significant trend at the 95% confidence level.

Interactions between WUE and plant growth did not bias the interpretation of the results presented here. For example, the combined effect of WUE and plant growth computed from the (Control − Constant CO_2) CLM5 experiment is −24.6 ± 1.3 mm/year, which is nearly the same as the summation of their contributions individually as follows: WUE = 42.4 ± 3.8 mm/year and plant growth = −67.0 ± 4.9 mm/year. Similarly, the combined effects of land-use change and irrigation (Control − no LU) (Figure 12, CLM5) similar to the summation of their contributions individually (Figure 9).

A quantitative comparison with the AVHHR-based LAI data from Boston University and for the limited period (1982 to 2010) shows that CLM5 overestimates the observed LAI trend in the SE US (Figure 13). The CLM5 simulated LAI trend is 0.13 m^2/m^2 per decade (p value <0.05), and AVHHR-LAI is 0.03 m^2/m^2 per decade (p value = 0.11). The LAI and NDVI show a similar trend, likely because LAI is a derived product from the NDVI data (Zhu et al., 2013).

We also assessed whether or not the simulated plant growth is consistent with observations. Observations for NDVI are available only from 1982 to the present. Figure 14 shows tshe NDVI trend (1982 to 2015) from the satellite observations. The NDVI has increased significantly in winter and fall seasons. Some areas also show an increasing trend in the spring season. NDVI did not increase significantly in the summer season, likely due to water limitation in the summer (Buermann et al., 2018). The main agricultural region – the Lower Mississippi River Valley shows a decreasing trend in spring and fall likely to be associated with crop planting and harvesting and an increasing trend in the summer that is likely associated with

irrigation effects. Overall, the observed NDVI trends are consistent with model-simulated trends (Figure 13), at least in their sign of change, i.e., increasing effect due in plant's growth in the forested area, and decreasing effect due to land-use change.

Finally, we assess the effect of each driver on seasonal cycle of LAI and runoff from the CLM single factor experiments (Figs. 14 and 15). Land-use change and plant's growth have the highest impacts on LAI seasonal cycle, where as effects due to climate change, irrigation, and WUE are one-order less than the land-use and plant growth's impact (Fig. 14). The LAI decreases due to land use change towards the end of crop growing season., that is, through July to October, that can be due to harvesting of the crops Plant growth increases the LAI in all seasons, with the highest increase found in the late spring and early summer season.

The climate impacts decrease runoff during the dry season, i.e. fall, and increase runoff in wet season, i.e. spring. Land-use change increases water availability all through the year with the highest increase in the winter season. Irrigation negatively impacts the runoff in the summer. The WUE increases runoff all through the year with the highest impact during the winter. Plant's growth shows a negative impact on water availability all through the year with the higest decrease in the winter. Our seasonal analysis can be further compared with the observational data.

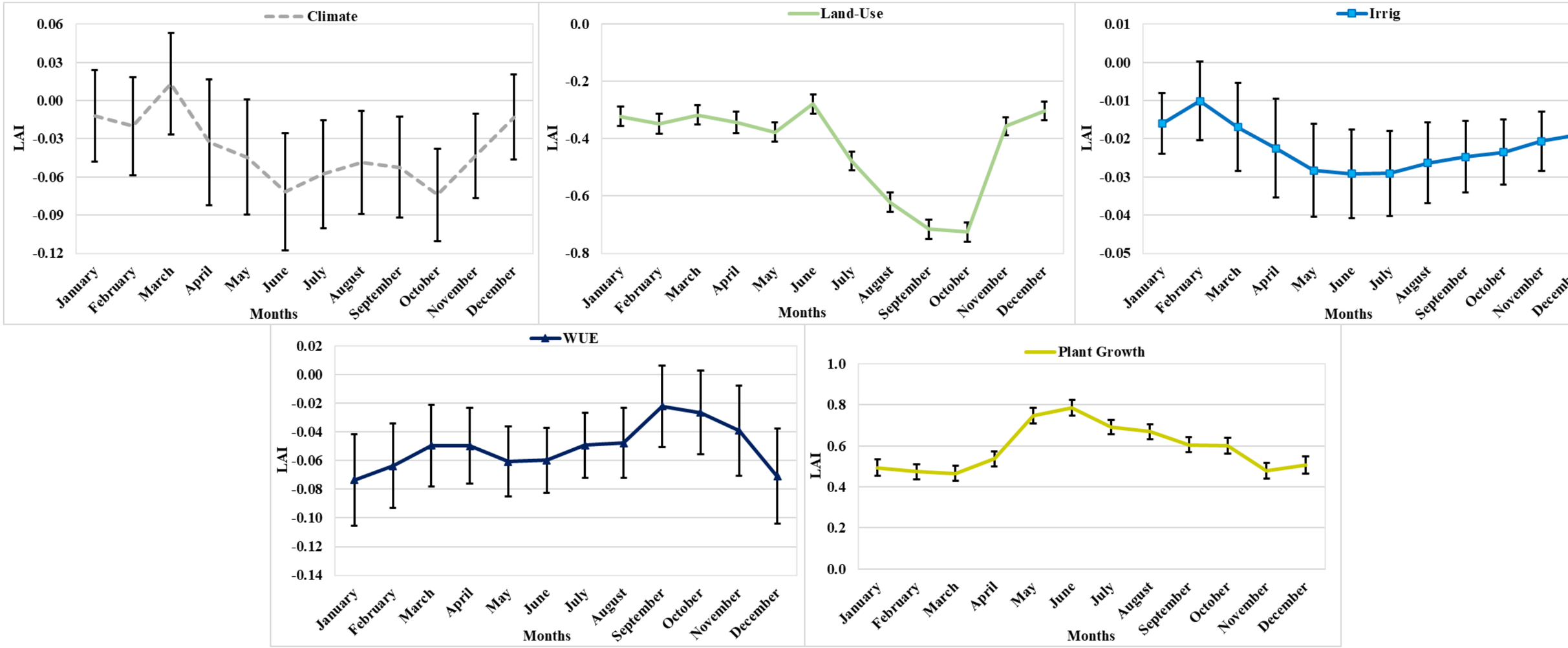

Figure 14. Monthly climatology in CLM5 LAI change from 1951 to 2010 showing the impacts of climate, land use change, irrigation, water use efficiency, and plant growth. Error bars show standard error.

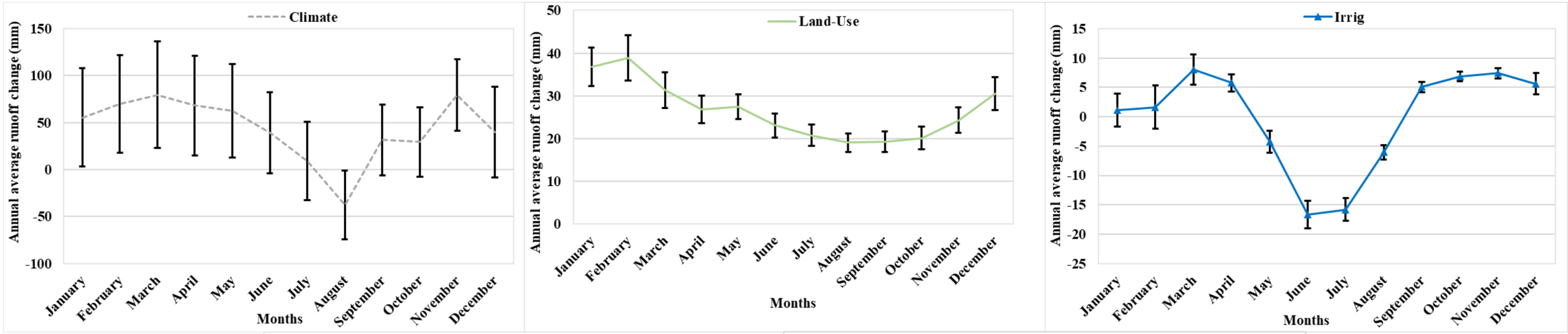

Figure 15. Monthly climatology in CLM5 runoff change from 1951 to 2010 showing the impacts of climate, land use change, irrigation, water use efficiency, and plant growth. Error bars show standard error.

3.4 Discussion and Conclusions

We diagnosed relative contributions of climate change (temperature and precipitation), land-use change, irrigation, increased WUE, and plant growth due to elevated CO_2 concentration on regional-scale hydrology of the Southeastern United States. We found that increase in runoff due to WUE (Swann et al., 2016) have been completely counteracted by the plant growth in the SE US. The effects of land-use change, and irrigation were small, mainly because of their smaller footprint in the SE US (Kumar, Merwade, et al., 2013). This result can change in intensive land-use change regions, for example, the Midwestern United States or highly irrigated region, for example, California Central Valley.

Figure A1 shows a global analysis of the contributions by the individual drivers to runoff change. The plant growth reduces runoff strongly in the subtropics, for example, SE US and La-Plata river basin in South America than the tropics, for example, the Amazon. The land-use change increases runoff in the Midwestern US. Dudley, et al., (2020) found an increasing streamflow trend in the agricultural watersheds of the Midwestern US and using USGS observations. The irrigation reduces runoff in dry regions, for example, Western North America and Central Asia. Caution is warranted in interpreting the climate impacts that can be biased due to the experiment design (Table 2). Our process-oriented methodology can be used to understand the drivers of the observed hydrological changes and uncertainties in future projections.

Satellite-based observations show that Earth's terrestrial surface is greening due to increased plant growth associated with elevated CO_2 (Zeng et al., 2018; Zhu et al., 2016). We show that Earth's greening can also play an important role in changing regional hydrology. We found that increased plant growth counteracts the effects of the increased WUE on water

availability in the Southeast. Compared with the direct human intervention in the hydrologic system, for example, changing land use and water management, the impact of the greening is not as easily visible to society. However, our results show that this relatively less known and slowly moving driver can play a substantial role in the water cycle of the humid and densely vegetated region. In future climate, plant growth can be limited due to water stress in the dry climate (Buermann et al., 2018; Kumar et al., 2016), and also due to nutrient (nitrogen and phosphorous) availability in the soil (Lombardozzi et al., 2015; Thornton et al., 2005).

Chapter 4. Summary and Conclusions

A study on long term drivers of hydrological changes in the Southeastern United States is presented in this thesis. The observational streamflow data has been used to analyze the long-term trends, followed by the use of process-based state-of-the-art global climate model Community Land Model version 5 (CLM5) to disentangle the drivers. The following conclusions are drawn from this study: I draw the following conclusions based on my study.

1. Vegetation decreases water availability in this region due to high evapotranspiration rates.
2. CLM control experiment and USGS observations show no significant trend in streamflow from 1951 to 2015 in the Southeast US.
3. Based on the analysis presented here, we conclude that the effect of CO_2 fertilization on plant growth can nullify the increasing water availability effects due to water use efficiency and land-use change effects.
4. Multi-model mean shows the cancelation of the increasing water availability due to WUE by the plant growth. Also, all four CMIP6 LUMIP models show an increase in LAI due to elevated CO_2 concentration in the atmosphere

While the results presented in the thesis are specific to the Southeastern US, the model (CLM5) and methodology used in this study illustrate that vegetation can have a large impact on streamflow in humid regions such as the SE US. This result can be extended to other studies including future water trends in the region and understanding the water dynamics in other parts of the United States.

APPENDIX

Table A1: List of 42 reference USGS stations included in the analysis.

FID	Gage ID	LAT	LON	STATION	AREA (SQ. KM.)
1	2361000	31.34	-85.61	CHOCTAWHATCHEE RIVER NEAR NEWTON, AL.	1781.61
2	2371500	31.57	-86.25	CONECUH RIVER AT BRANTLEY AL	1292.79
3	2374500	31.42	-86.99	MURDER CREEK NEAR EVERGREEN AL	445.72
4	2467500	32.57	-88.19	SUCARNOOCHEE RIVER AT LIVINGSTON AL	1574.12
5	3574500	34.62	-86.31	PAINT ROCK RIVER NEAR WOODVILLE AL	813.80
6	7056000	35.98	-92.75	BUFFALO RIVER NEAR ST. JOE, AR	2149.36
7	7252000	35.58	-94.02	MULBERRY RIVER NEAR MULBERRY. AR	968.99
8	2231000	30.36	-82.08	ST. MARYS RIVER NEAR MACCLENNY, FL	1748.37
9	2315500	30.33	-82.74	SUWANNEE RIVER AT WHITE SPRINGS, FLA.	6136.26
10	2324000	29.79	-83.32	STEINHATCHEE RIVER NEAR CROSS CITY, FLA.	791.02
11	2326000	30.17	-83.82	ECONFINA RIVER NEAR PERRY, FLA.	556.41
12	2245500	29.98	-81.85	SOUTH FORK BLACK CREEK NEAR PENNEY FARMS, FL	348.43
13	2296500	27.38	-81.80	CHARLIE CREEK NEAR GARDNER FL	886.40

14	2246000	30.11	-81.91	NORTH FORK BLACK CREEK NEAR MIDDLEBURG, FL	451.06
15	2297310	27.20	-81.99	HORSE CREEK AT SR 72 NEAR ARCADIA, FL	528.38
16	2314500	30.68	-82.56	SUWANNEE RIVER AT US 441, AT FARGO, GA	3322.15
17	2228500	30.52	-82.23	NORTH PRONG ST. MARYS RIVER AT MONIAC, GA	496.95
18	7373000	31.54	-92.41	BIG CREEK AT POLLOCK, LA	131.18
19	7375000	30.62	-90.25	TCHEFUNCTE RIVER NEAR FOLSOM, LA	249.35
20	7376000	30.50	-90.68	TICKFAW RIVER AT HOLDEN, LA	651.61
21	7376500	30.50	-90.55	NATALBANY RIVER AT BAPTIST, LA	205.19
22	7377000	30.89	-90.84	AMITE RIVER NEAR DARLINGTON, LA	1525.31
23	8013000	31.00	-92.67	CALCASIEU RIVER NR GLENMORA, LA	1293.69
24	8014500	30.70	-92.89	OUISKA CHITTO CREEK NEAR OBERLIN, LA	1305.15
25	2472000	31.71	-89.41	LEAF RIVER NR COLLINS, MS	1927.13
26	2472500	31.43	-89.41	BOUIE CREEK NR HATTIESBURG, MS	789.94
27	7291000	31.50	-90.78	HOMOCHITTO RIVER AT EDDICETON, MS	479.30
28	2108000	34.83	-77.83	NORTHEAST CAPE FEAR RIVER NEAR CHINQUAPIN, NC	1569.49
29	2111500	36.18	-81.17	REDDIES RIVER AT NORTH WILKESBORO, NC	233.66

30	2070500	36.53	-79.99	MAYO RIVER NEAR PRICE, NC	672.64
31	2081500	36.19	-78.58	TAR RIVER NEAR TAR RIVER, NC	428.37
32	2143000	35.68	-81.40	HENRY FORK NEAR HENRY RIVER, NC	216.67
33	3161000	36.39	-81.41	SOUTH FORK NEW RIVER NEAR JEFFERSON, NC	527.86
34	3439000	35.14	-82.82	FRENCH BROAD RIVER AT ROSMAN, NC	178.67
35	3441000	35.27	-82.71	DAVIDSON RIVER NEAR BREVARD, NC	104.29
36	3450000	35.65	-82.41	BEETREE CREEK NEAR SWANNANOA, NC	14.08
37	3460000	35.67	-83.07	CATALOOCHEE CREEK NEAR CATALOOCHEE, NC	127.02
38	3479000	36.24	-81.82	WATAUGA RIVER NEAR SUGAR GROVE, NC	235.60
39	3500000	35.15	-83.38	LITTLE TENNESSEE RIVER NEAR PRENTISS, NC	361.14
40	3504000	35.13	-83.62	NANTAHALA RIVER NEAR RAINBOW SPRINGS, NC	134.52
41	3465500	36.18	-82.46	NOLICHUCKY RIVER AT EMBREEVILLE, TN	2081.60
42	3604000	35.50	-87.83	BUFFALO RIVER NEAR FLAT WOODS, TN	1163.03

Figure A1: A global analysis of the drivers of hydrological changes from 1951 to 2015 and CLM5 experiments. Unit: % changes: e.g., WUE effects: (Control – Stomatal Conductance Constant CO_2) *100/Control. We have used a control experiment in the denominator for % change calculation in all experiments and consistency purposes.

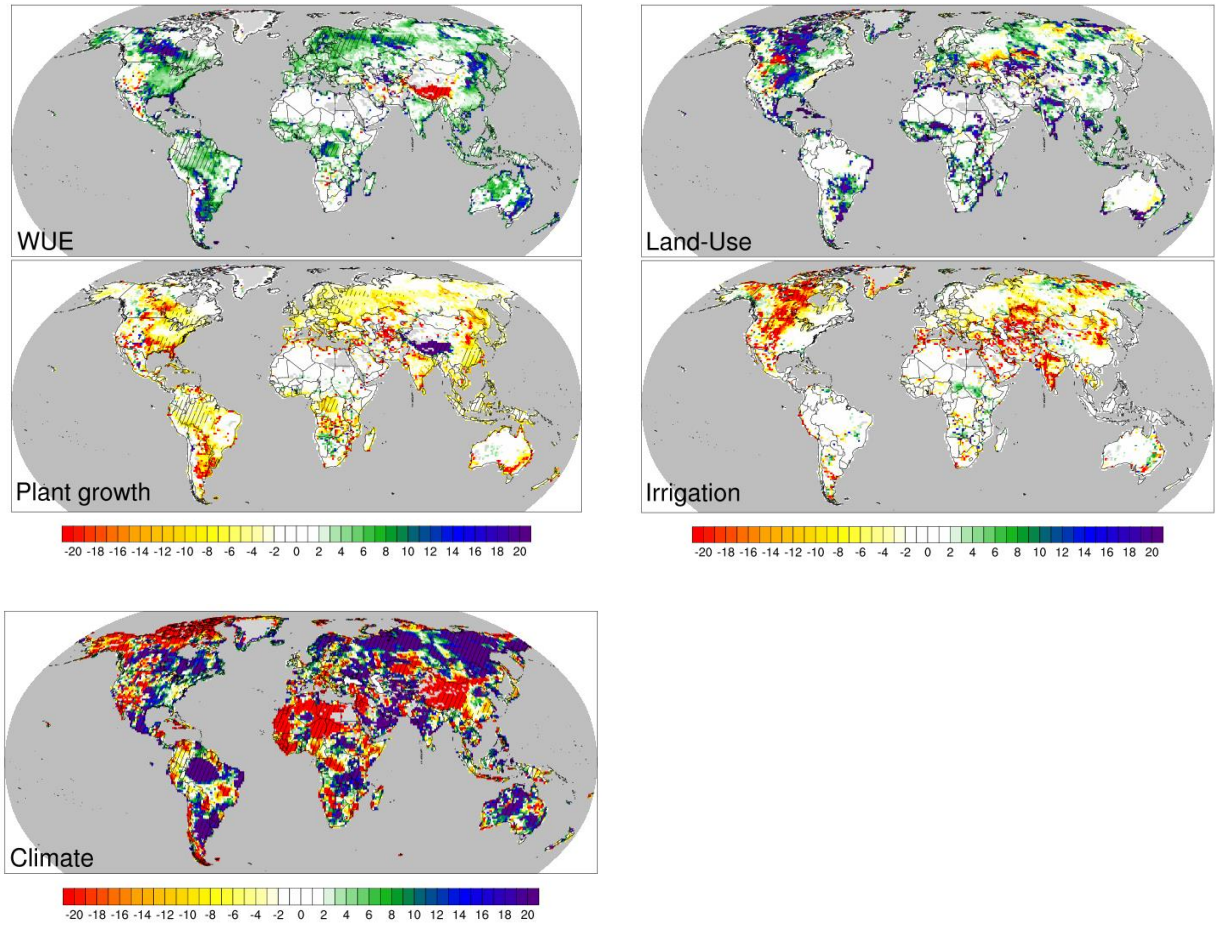

Figure A2: United States temperature trend from 1951 to 2015 and GISS data. Unit: ºC /decade. Blue box shows the Southeastern United States showing non-significant changes in temperature.

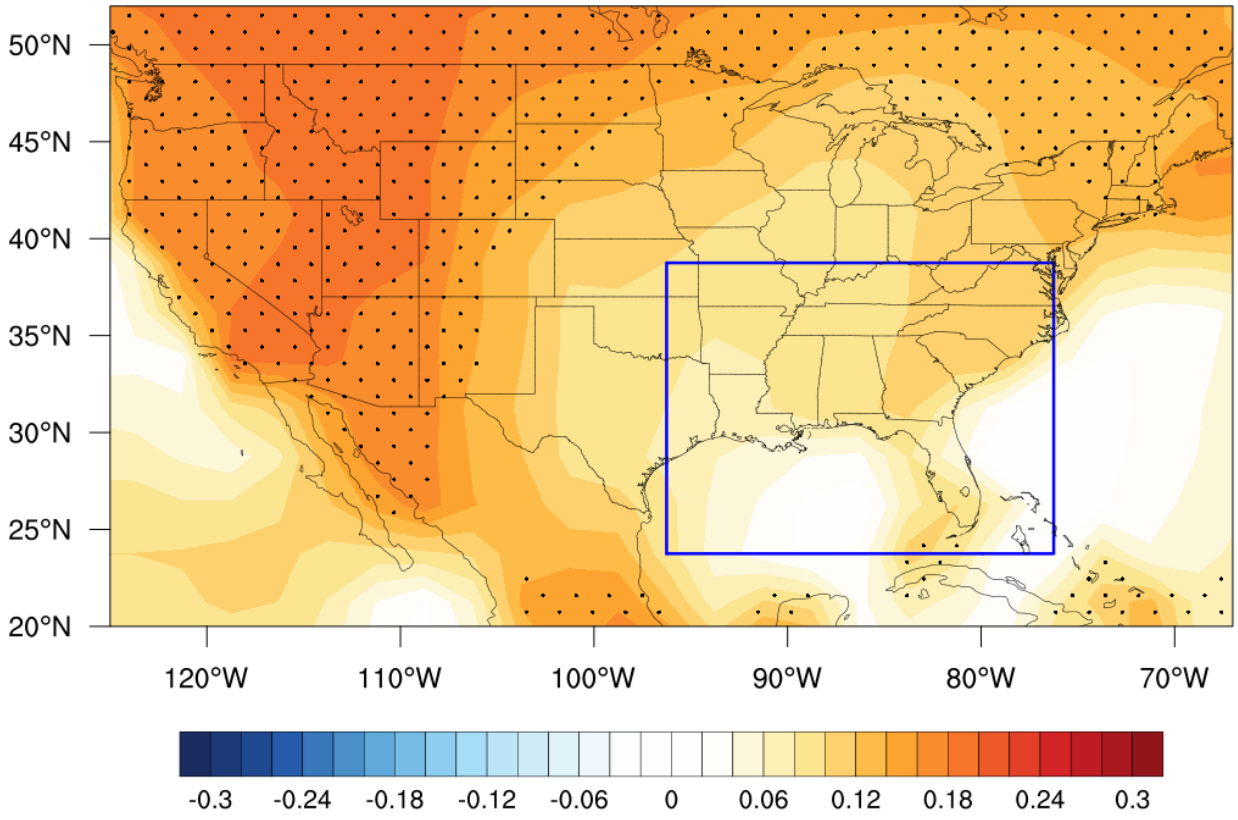

REFERENCES

Ainsworth, E. A., & Long, S. P. (2005). What have we learned from 15 years of free-air CO2 enrichment (FACE)? A meta-analytic review of the responses of photosynthesis, canopy properties and plant production to rising CO2. *New Phytologist*, *165*(2), 351–372. https://doi.org/10.1111/j.1469-8137.2004.01224.x

Allan, R. P. (2014). Dichotomy of drought and deluge. *Nature Geoscience*, *7*(10), 700–701. https://doi.org/10.1038/ngeo2243

Alston, J. M., Babcock, B. A., & Pardey, P. G. (2010). The Shifting Patterns of Agricultural Production and Productivity Worldwide. In *The Midwest Agribusiness Trade Research and Information Center, Iowa State UNiversity, Ames, Iowa* (Vol. 33). https://doi.org/10.1073/pnas.0703993104

Bonan, G. B. (2016). *Ecological climatology: concepts and applications* (Third Edit). https://doi.org/10.5860/choice.40-3988

Bonan, G. B., Lawrence, P. J., Oleson, K. W., Levis, S., Jung, M., Reichstein, M., … Swenson, S. C. (2011). Improving canopy processes in the Community Land Model version 4 (CLM4) using global flux fields empirically inferred from FLUXNET data. *Journal of Geophysical Research*, *116*(G2), 1–22. https://doi.org/10.1029/2010jg001593

Budyko, M. I. (1958). *The Heat Balance of Earth's Surface*. US Department of Commerce, Washington, DC.

Buermann, W., Forkel, M., O'Sullivan, M., Sitch, S., Friedlingstein, P., Haverd, V., … Richardson, A. D. (2018). Widespread seasonal compensation effects of spring warming on northern plant productivity. *Nature*, *562*(7725), 110–114. https://doi.org/10.1038/s41586-018-0555-7

Chang, E. K. M., Zheng, C., Lanigan, P., Yau, A. M. W., & Neelin, J. D. (2015). Significant modulation of variability and projected change in California winter precipitation by extratropical cyclone activity. *Geophysical Research Letters*, *42*(14), 5983–5991. https://doi.org/10.1002/2015GL064424

Charney, B. J. G. (1975). Dynamics of deserts and drought in the Sahel. *Quart. J. R. Met. SOC*, *101*(March 1974), 193–202.

Collatz, G., Ribas-Carbo, M., & Berry, J. (1992). Coupled Photosynthesis-Stomatal Conductance Model for Leaves of C4 Plants. *Functional Plant Biology*, *19*(5), 519. https://doi.org/10.1071/pp9920519

Cook, B. I., Mankin, J. S., & Anchukaitis, K. J. (2018). Climate Change and Drought: From Past to Future. *Current Climate Change Reports*, *4*(2), 164–179. https://doi.org/10.1007/s40641-018-0093-2

Crow, W. T., & Yilmaz, M. T. (2014). The auto-tuned land data assimilation system (ATLAS). *Water Resources Research*, *50*(1), 371–385. https://doi.org/10.1002/2013WR014550

Dai, A. (2013). Increasing drought under global warming in observations and models. *Nature Climate Change*, *3*(1), 52–58. https://doi.org/10.1038/nclimate1633

Daly, C., Halbleib, M., Smith, J., Gibson, W., Dogget, M., Taylor, G., … Pasteris, P. (2008). Physiographically sensitive mapping of climatological temperature and precipitation across the conterminous United States. *International Journal of Climatology*, *28*(March 2008), 2031–2064. https://doi.org/10.1002/joc

Daly, C., Neilson, R., & Phillips, D. L. (1994). A statistical-topographic model for mapping climatological precipitation over mountainous terrain. *Journal of Applied Meteorology*, *33*, 140–158.

Dang, Q. L., Margolis, H. A., & Collatz, G. J. (1998). Parameterization and testing of a coupled photosynthesis-stomatal conductance model for boreal trees. *Tree Physiology*, *18*(3), 141–153. https://doi.org/10.1093/treephys/18.3.141

Dawes, W., Ali, R., Varma, S., Emelyanova, I., Hodgson, G., & McFarlane, D. (2012). Modelling the effects of climate and land cover change on groundwater recharge in south-west Western Australia. *Hydrology and Earth System Sciences*, *16*(8), 2709–2722. https://doi.org/10.5194/hess-16-2709-2012

De Noblet-Ducoudré, N., Boisier, J. P., Pitman, A., Bonan, G. B., Brovkin, V., Cruz, F., … Voldoire, A. (2012). Determining robust impacts of land-use-induced land cover changes on surface climate over North America and Eurasia: Results from the first set of LUCID experiments. *Journal of Climate*, *25*(9), 3261–3281. https://doi.org/10.1175/JCLI-D-11-00338.1

Donohue, R. J., Roderick, M. L., & McVicar, T. R. (2012). Roots, storms and soil pores: Incorporating key ecohydrological processes into Budyko's hydrological model. *Journal of Hydrology*, *436–437*, 35–50. https://doi.org/10.1016/j.jhydrol.2012.02.033

Donohue, R. J., Roderick, M. L., McVicar, T. R., & Farquhar, G. D. (2013). Impact of CO2 fertilization on maximum foliage cover across the globe's warm, arid environments. *Geophysical Research Letters*, *40*(12), 3031–3035. https://doi.org/10.1002/grl.50563

Dudley, R. W., Hirsch, R. M., Archfield, S. A., Blum, A. G., & Renard, B. (2020). Low streamflow trends at human-impacted and reference basins in the United States. *Journal of Hydrology*, *580*(April 2019), 124254. https://doi.org/10.1016/j.jhydrol.2019.124254

Eberts, S. M., Woodside, M. D., Landers, M. N., & Wagner, C. R. (2019). *Monitoring the Pulse of Our Nation's Rivers and Streams: The US Geological Survey Streamgaging Network*

Unique Partnership A Network of Networks National Streamflow Network (NSN). https://doi.org/10.3133/fs20183081

Eyring, V., Bony, S., Meehl, G. A., Senior, C. A., Stevens, B., Stouffer, R. J., & Taylor, K. E. (2016). Overview of the Coupled Model Intercomparison Project Phase 6 (CMIP6) experimental design and organization. *Geoscientific Model Development*, *9*(5), 1937–1958. https://doi.org/10.5194/gmd-9-1937-2016

Falcone, J. et al. (2011). *GAGES II (Geospatial Attributes of Gages for Evaluating Streamflow) sumary report*. https://doi.org/https://water.usgs.gov/GIS/dsdl/basinchar_and_ report_sept_2011.zip

Falcone, J. A., Carlisle, D. M., Wolock, D. M., & Meador, M. R. (2010). GAGES: A stream gage database for evaluating natural and altered flow conditions in the conterminous United States. *Ecology*, *91*(2), 621–621. https://doi.org/10.1890/09-0889.1

Farquhar, G. D., von Caemmerer, S., & Berry, J. A. (1980). A biochemical model of photosynthetic CO<Subscript>2</Subscript> assimilation in leaves of C<Subscript>3</Subscript> species. *Planta*, *149*(1), 78–90. Retrieved from https://link.springer.com/article/10.1007/BF00386231%0Apapers3://publication/doi/10.1007/BF00386231

Forkel, M., Carvalhais, N., Rödenbeck, C., Keeling, R., Heimann, M., Thonicke, K., … Reichstein, M. (2016). Enhanced seasonal CO2 exchange caused by amplified plant productivity in northern ecosystems. *Science*, *351*(6274), 696–699. https://doi.org/10.1126/science.aac4971

Fowler, M. D., Kooperman, G. J., Randerson, J. T., & Pritchard, M. S. (2019). The effect of plant physiological responses to rising CO2 on global streamflow. *Nature Climate Change*,

9(11), 873–879. https://doi.org/10.1038/s41558-019-0602-x

Frank, D. C., Poulter, B., Saurer, M., Esper, J., Huntingford, C., Helle, G., … Weigl, M. (2015). Water-use efficiency and transpiration across European forests during the Anthropocene. *Nature Climate Change*, *5*(6), 579–583. https://doi.org/10.1038/nclimate2614

Fu, B. P. (1981). On the calculation of the evaporation from the land surface. *Sci. Atmos. Sin. (in Chinese)*, 23–31.

Gornitz, V., Rosenzweig, C., & Hillel, D. (1997). Effects of anthropogenic intervention in the land hydrologic cycle on global sea level rise. *Global and Planetary Change*, *14*(3–4), 147–161. https://doi.org/10.1016/S0921-8181(96)00008-2

Gray, S. B., Dermody, O., Klein, S. P., Locke, A. M., McGrath, J. M., Paul, R. E., … Leakey, A. D. B. (2016). Intensifying drought eliminates the expected benefits of elevated carbon dioxide for soybean. *Nature Plants*, *2*(September). https://doi.org/10.1038/nplants.2016.132

Greve, P., Orlowsky, B., Mueller, B., Sheffield, J., Reichstein, M., & Seneviratne, S. I. (2014). Global assessment of trends in wetting and drying over land. *Nature Geoscience*, *7*(10), 716–721. https://doi.org/10.1038/ngeo2247

Hamed, K. H. (2008). Trend detection in hydrologic data: The Mann-Kendall trend test under the scaling hypothesis. *Journal of Hydrology*, *349*(3–4), 350–363. https://doi.org/10.1016/j.jhydrol.2007.11.009

Held, I., & Soden, B. J. (2006). on the Joint Estimation of Unknown Parameters and Disturbances in Linear Stochastic Time-Variant Systems. *Journal of Climate*, *19*, 5686–5699. https://doi.org/10.5220/0001648603850388

Idso, S. B., & Kimball, B. A. (1992). Effects of long-term atmospheric CO2 enrichment on the growth and fruit production of sour orange trees. *Plant Physiology*, *99*, 341–343.

https://doi.org/10.1046/j.1365-2486.1997.00053.x

Kendall, M. G. (1975). *Rank Correlation Methods* (4th Editio). https://doi.org/10.4236/ns.2014.61003

Kinal, J., & Stoneman, G. L. (2012). Disconnection of groundwater from surface water causes a fundamental change in hydrology in a forested catchment in south-western Australia. *Journal of Hydrology*, *472–473*, 14–24. https://doi.org/10.1016/j.jhydrol.2012.09.013

Koster, R. D., & Suarez, M. J. (1999). A simple framework for examining the interannual variability of land surface moisture fluxes. *Journal of Climate*, *12*(7), 1911–1917. https://doi.org/10.1175/1520-0442(1999)012<1911:ASFFET>2.0.CO;2

Koutsoyiannis, D., & Montanari, A. (2007). Statistical analysis of hydroclimatic time series: Uncertainty and insights. *Water Resources Research*, *43*(5), 1–9. https://doi.org/10.1029/2006WR005592

Kumar, S., Allan, R. P., Zwiers, F., Lawrence, D. M., & Dirmeyer, P. A. (2015). Limitations Over Land. *Geophysical Research Letters*, *42*, 10,867-10,875. https://doi.org/10.1002/2015GL066858.Received

Kumar, S., Kinter, J., Dirmeyer, P. A., Pan, Z., & Adams, J. (2013). Multidecadal climate variability and the "warming hole" in north america: Results from CMIP5 twentieth- and twenty-first-century climate simulations. *Journal of Climate*, *26*(11), 3511–3527. https://doi.org/10.1175/JCLI-D-12-00535.1

Kumar, S., Lawrence, D. M., Dirmeyer, P. A., & Sheffield, J. (2013). Earth' s Future Less reliable water availability in the 21st century climate projections Earth' s Future. *Earth's Future*, *2*, 152–160. https://doi.org/10.1002/2013EF000159.Abstract

Kumar, S., Merwade, V., Kam, J., & Thurner, K. (2009). Streamflow trends in Indiana: Effects

of long term persistence, precipitation and subsurface drains. *Journal of Hydrology*. https://doi.org/10.1016/j.jhydrol.2009.06.012

Kumar, S., Merwade, V., Rao, P. S. C., & Pijanowski, B. C. (2013). Characterizing long-term land use/cover change in the United States from 1850 to 2000 using a nonlinear bi-analytical model. *Ambio*, *42*(3), 285–297. https://doi.org/10.1007/s13280-012-0354-6

Kumar, S., Newman, M., Lawrence, D. M., Lo, M.-H., Akula, S., Lan, C.-W., … Lombardozzi, D. (2020). The GLACE-Hydrology Experiment: Effects of Land-Atmosphere Coupling on Soil Moisture Variability and Predictability. *Journal of Climate*. https://doi.org/10.1175/jcli-d-19-0598.1

Kumar, S., Zwiers, F., Dirmeyer, P. A., Lawrence, D. M., Shrestha, R., & Werner, A. T. (2016). Terrestrial contribution to the heterogeneity in hydrological changes under global warming. *Water Resources Research*, *51*, 9127–9140. https://doi.org/10.1002/2014WR016259

Langenbrunner, B., Neelin, J. D., Lintner, B. R., & Anderson, B. T. (2015). Patterns of precipitation change and climatological uncertainty among CMIP5 models, with a focus on the midlatitude pacific storm track. *Journal of Climate*, *28*(19), 7857–7872. https://doi.org/10.1175/JCLI-D-14-00800.1

Lawrence, D. M., Fisher, R. A., Koven, C. D., Oleson, K. W., Swenson, S. C., Bonan, G., … Lipscomb, W. H. (2019). The Community Land Model version 5: Description of new features, benchmarking, and impact of forcing uncertainty. *Journal of Advances in Modeling Earth Systems*.

Lawrence, D. M., Hurtt, G. C., Arneth, A., Brovkin, V., Calvin, K. V., Jones, A. D., … Shevliakova, E. (2016). The Land Use Model Intercomparison Project (LUMIP) contribution to CMIP6: Rationale and experimental design. *Geoscientific Model*

Development, *9*(9), 2973–2998. https://doi.org/10.5194/gmd-9-2973-2016

Lehner, F., Wood, A. W., Vano, J. A., Lawrence, D. M., Clark, M. P., & Mankin, J. S. (2019). Runoff Projections From Climate Models. *Nature Climate Change*, *9*(December). https://doi.org/10.1038/s41558-019-0639-x

Lemordant, L., Gentine, P., Swann, A. S., Cook, B. I., & Scheff, J. (2018). Critical impact of vegetation physiology on the continental hydrologic cycle in response to increasing CO 2 . *Proceedings of the National Academy of Sciences*, *115*(16), 4093–4098. https://doi.org/10.1073/pnas.1720712115

Li, D., Pan, M., Cong, Z., Zhang, L., & Wood, E. (2013). Vegetation control on water and energy balance within the Budyko framework. *Water Resources Research*, *49*(2), 969–976. https://doi.org/10.1002/wrcr.20107

Li, Q., Wei, X., Zhang, M., Liu, W., Fan, H., Zhou, G., … Wang, Y. (2017). Forest cover change and water yield in large forested watersheds: A global synthetic assessment. *Ecohydrology*, *10*(4), 1–7. https://doi.org/10.1002/eco.1838

Liu, N., Harper, R. J., Smettem, K. R. J., Dell, B., & Liu, S. (2019a). Responses of streamflow to vegetation and climate change in southwestern Australia. *Journal of Hydrology*, *572*(September 2018), 761–770. https://doi.org/10.1016/j.jhydrol.2019.03.005

Liu, N., Harper, R. J., Smettem, K. R. J., Dell, B., & Liu, S. (2019b). Responses of streamflow to vegetation and climate change in southwestern Australia. *Journal of Hydrology*. https://doi.org/10.1016/j.jhydrol.2019.03.005

Livneh, B., & Hoerling, M. P. (2016). The physics of drought in the US Central Great Plains. *Journal of Climate*, *29*(18), 6783–6804. https://doi.org/10.1175/JCLI-D-15-0697.1

Lombardozzi, D. L., Bonan, G. B., Levis, S., & Lawrence, D. M. (2018). Changes in Wood

Biomass and Crop Yields in Response to Projected CO2, O3, Nitrogen Deposition, and Climate. *Journal of Geophysical Research: Biogeosciences*, *123*(10), 3262–3282. https://doi.org/10.1029/2018JG004680

Mahmood, R., Pielke, R. A., Hubbard, K. G., Niyogi, D., Dirmeyer, P. A., Mcalpine, C., … Fall, S. (2014). Land cover changes and their biogeophysical effects on climate. *International Journal of Climatology*, *34*(4), 929–953. https://doi.org/10.1002/joc.3736

Mankin, J. S., Seager, R., Smerdon, J. E., Cook, B. I., & Williams, A. P. (2019). Mid-latitude freshwater availability reduced by projected vegetation responses to climate change. *Nature Geoscience*, *12*(12), 983–988. https://doi.org/10.1038/s41561-019-0480-x

Mann, H. B. (1945). Nonparametric Tests Against Trend. *Econometrica*, *13*(3), 245–259. Retrieved from https://www.jstor.org/stable/1907187

Massey, J. H., Mark Stiles, C., Epting, J. W., Shane Powers, R., Kelly, D. B., Bowling, T. H., … Pennington, D. A. (2017). Long-term measurements of agronomic crop irrigation made in the Mississippi delta portion of the lower Mississippi River Valley. *Irrigation Science*, *35*(4), 297–313. https://doi.org/10.1007/s00271-017-0543-y

McNider, R., & Christy, J. (2007). Let the East Bloom Again. *New York Times Op-Ed*, 8–10. Retrieved from http://www.nytimes.com/2007/09/22/opinion/22mcnider.html

Medlyn, B. E., Duursma, R. A., Eamus, D., Ellsworth, D. S., Prentice, I. C., Barton, C. V. M., … Wingate, L. (2011). Reconciling the optimal and empirical approaches to modelling stomatal conductance. *Global Change Biology*, *17*(6), 2134–2144. https://doi.org/10.1111/j.1365-2486.2010.02375.x

Meehl, G. A., Arblaster, J. M., & Chung, C. T. Y. (2015). Dissapearance of the southeast US "warming hole" with the late 1990's transition of the Interdecadal Pacific Oscillation.

Geophysical Research Letters, *42*, 5564–5570. https://doi.org/10.1002/2015GL064586.Received

Meehl, G. A., & Tebaldi, C. (2004). More intense, more frequent, and longer lasting heat waves in the 21st century. *Science*, *305*(5686), 994–997. https://doi.org/10.1126/science.1098704

Misra, K. G., Yadav, R. R., & Misra, S. (2015). Satluj river flow variations since AD 1660 based on tree-ring network of Himalayan cedar from western Himalaya, India. *Quaternary International*, *371*(January 2019), 135–143. https://doi.org/10.1016/j.quaint.2015.01.015

Mitchell, T. D., & Jones, P. D. (2005). An improved method of constructing a database of monthly climate observations and associated high-resolution grids. *International Journal of Climatology*, *25*(6), 693–712. https://doi.org/10.1002/joc.1181

Monteith, J. L. (1965). Evaporation and Environment. *Symposia of the Society for Experimental Biology*, *19*, 205–234.

Myneni, R. B., Keeling, C. D., Tucker, C. J., Asrar, G., & Nemani, R. R. (1997). Increased plant growth in the northern high latitudes from 1981 to 1991. *Nature*, *386*(6626), 698–702. https://doi.org/10.1038/386698a0

Nagy, R. C., Lockaby, B. G., Helms, B., Kalin, L., & Stoeckel, D. (2011). Water Resources and Land Use and Cover in a Humid Region: The Southeastern United States. *Journal of Environment Quality*, *40*(3), 867. https://doi.org/10.2134/jeq2010.0365

Napton, D. E., Auch, R. F., Headley, R., & Taylor, J. L. (2010). Land changes and their driving forces in the Southeastern United States. *Regional Environmental Change*, *10*(1), 37–53. https://doi.org/10.1007/s10113-009-0084-x

Newman, M., Alexander, M. A., Ault, T. R., Cobb, K. M., Deser, C., Di Lorenzo, E., … Smith, C. A. (2016). The Pacific decadal oscillation, revisited. *Journal of Climate*, *29*(12), 4399–

4427. https://doi.org/10.1175/JCLI-D-15-0508.1

Önöz, B., & Bayazit, M. (2003). The power of statistical tests for trend detection. *Turkish Journal of Engineering and Environmental Sciences*, *27*(4), 247–251. https://doi.org/10.3906/sag-1205-120

Padrón, R. S., Gudmundsson, L., Greve, P., & Seneviratne, S. I. (2017). Large-Scale Controls of the Surface Water Balance Over Land: Insights From a Systematic Review and Meta-Analysis. *Water Resources Research*, *53*(11), 9659–9678. https://doi.org/10.1002/2017WR021215

Pan, Z., Liu, X., Kumar, S., Gao, Z., & Kinter, J. (2013). Intermodel variability and mechanism attribution of central and southeastern US anomalous cooling in the twentieth century as simulated by CMIP5 models. *Journal of Climate*, *26*(17), 6215–6237. https://doi.org/10.1175/JCLI-D-12-00559.1

Penman, H. L. (1948). Natural evapotranspiration from open water, bare soil and grass. *Proceedings of the Royal Society of London. Series A, Mathematical and Physical Sciences*, *193*(1032), 120–145. https://doi.org/10.1007/s13398-014-0173-7.2

Qi, W., Liu, J., & Leung, F. (2019). A framework to quantify impacts of elevated CO 2 concentration, global warming and leaf area changes on seasonal variations of water resources on a river basin scale. *Journal of Hydrology*. https://doi.org/10.1016/j.jhydrol.2019.01.015

Roderick, M. L., & Farquhar, G. D. (2011). A simple framework for relating variations in runoff to variations in climatic conditions and catchment properties. *Water Resources Research*, *47*(6), 1–11. https://doi.org/10.1029/2010WR009826

Sayler, K. L., Acevedo, W., & Taylor, J. L. (2015). Status and trends of land change in the Great

Plains of the United States--1973 to 2000. *Professional Paper*. https://doi.org/10.3133/pp1794B

Sayler, Kristi L., Acevedo, W., & Taylor, J. L. (2016). Status and trends of land change in selected US ecoregions - 2000 to 2011. *Photogrammetric Engineering and Remote Sensing*, *82*(9), 687–697. https://doi.org/10.14358/PERS.82.9.687

Schaible, G. D., & Aillery, M. P. (2012). Water Conservation in Irrigated Agriculture: Trends and Challenges in the Face of Emerging Demands. *United States Department of Agriculture Economic Research Service Economic Information Bulletin*, (99). Retrieved from http://www.ers.usda.gov

Scheff, J., & Frierson, D. M. W. (2014). Scaling potential evapotranspiration with greenhouse warming. *Journal of Climate*, *27*(4), 1539–1558. https://doi.org/10.1175/JCLI-D-13-00233.1

Schilling, K. E. (2016). Comment on "Climate and agricultural land use change impacts on streamflow in the upper midwestern United States" by Satish C. Gupta et al. *Water Resources Research*, *52*(7), 5694–5696. https://doi.org/10.1111/j.1752-1688.1969.tb04897.x

Scott, D. F., & Prinsloo, F. W. (2009). Longer-term effects of pine and eucalypt plantations on streamflow. *Water Resources Research*, *45*(7), 1–8. https://doi.org/10.1029/2007WR006781

Seager, R., Tzanova, A., & Nakamura, J. (2009). Drought in the Southeastern United States: Causes, variability over the last millennium, and the potential for future hydroclimate change. *Journal of Climate*, *22*(19), 5021–5045. https://doi.org/10.1175/2009JCLI2683.1

Selman, C., & Misra, V. (2016). The sensitivity of southeastern United States climate to varying irrigation vigor. *Journal of Geophysical Research: Atmospheres*, *121*, 7606–7621.

https://doi.org/https://doi.org/10.1002/2016JD025002

Sen, P. K. (1968). Estimates of the Regression Coefficient Based on Kendall's Tau. *Journal of the American Statistical Association*, *63*(324), 1379–1389. https://doi.org/10.1080/01621459.1968.10480934

Sun, L., Yang, L., Hao, L., Fang, D., Jin, K., & Huang, X. (2017). Hydrological effects of vegetation cover degradation and environmental implications in a semiarid temperate Steppe, China. *Sustainability (Switzerland)*, *9*(2), 1–20. https://doi.org/10.3390/su9020281

Swank, W., Swift, J. L., & Douglass, J. (1988). *Streamflow changes associated with forest cutting, species conversions, and natural disturbances, in Forest hydrology and ecology at Coweeta*. Springer.

Swann, A. L. S., Hoffman, F. M., Koven, C. D., & Randerson, J. T. (2016). Plant responses to increasing CO2 reduce estimates of climate impacts on drought severity. *Proceedings of the National Academy of Sciences of the United States of America*, *113*(36), 10019–10024. https://doi.org/10.1073/pnas.1604581113

Tans, P. A., & Keeling, R. F. (2019). *Trends in Atmospheric Carbon Dioxide.* Retrieved from http://www.fsis.usda.gov/regulations/European_Union_Requirements/index.asp.

Theil, H. (1992). *A Rank-Invariant Method of Linear and Polynomial Regression Analysis*. *3*(1950), 345–381. https://doi.org/10.1007/978-94-011-2546-8_20

Thornton, P. E., Law, B. E., Gholz, H. L., Clark, K. L., Falge, E., Ellsworth, D. S., … Falk, M. (2002). Modeling and measuring the effects of disturbance history and climate on carbon and water budgets in evergreen needleleaf forests. *Agricultural and Forest Meteorology*, *113*(1–4), 185–222.

Thornton, Peter E., & Rosenbloom, N. A. (2005). Ecosystem model spin-up: Estimating steady

state conditions in a coupled terrestrial carbon and nitrogen cycle model. *Ecological Modelling*, *189*(1–2), 25–48. https://doi.org/10.1016/j.ecolmodel.2005.04.008

Trancoso, R., Larsen, J. R., McVicar, T. R., Phinn, S. R., & McAlpine, C. A. (2017). CO2-vegetation feedbacks and other climate changes implicated in reducing base flow. *Geophysical Research Letters*, *44*(5), 2310–2318. https://doi.org/10.1002/2017GL072759

Trimble, S. W. (2008). Man-induced soil erosion of the Southern Piedmont. In *Soil & Water Conservation Society, Ankeny, IA*. https://doi.org/10.1016/0305-7488(76)90171-7

Tucker, C. J., Fung, I. Y., Keeling, C. D., & Gammon, R. H. (1986). Relationship between atmospheric CO2 variations and a satellite-derived vegetation index. *Nature*, *319*(6050), 195–199. https://doi.org/10.1038/319195a0

Ukkola, A. M., Keenan, T. F., Kelley, D. I., & Prentice, I. C. (2016). Vegetation plays an important role in mediating future water resources. *Environmental Research Letters*, *11*(9), 0–8. https://doi.org/10.1088/1748-9326/11/9/094022

Vermote, E., Justice, C., Csiszar, I., J., E., & Myneni, R. B. et al. (2014). *NOAA Climate Data Record (CDR) of normalized Difference Vegetation Index (NDVI), Version 4, NOAA Natl. Clim. Data Cent.*

Viovy, N. (2011). *CRUNCEP dataset. [Description available at http://dods.extra.cea.fr/data/p529viov/cruncep/readme. htm. Data available at http://dods.extra.cea.fr/store/p529viov/cruncep/V4_1901_2011/].*

Wada, Y., Reager, J. T., Chao, B. F., Wang, J., Lo, M. H., Song, C., … Gardner, A. S. (2017). Recent Changes in Land Water Storage and its Contribution to Sea Level Variations. *Surveys in Geophysics*, *38*(1), 131–152. https://doi.org/10.1007/s10712-016-9399-6

Wada, Y., Van Beek, L. P. H., Van Kempen, C. M., Reckman, J. W. T. M., Vasak, S., &

Bierkens, M. F. P. (2010). Global depletion of groundwater resources. *Geophysical Research Letters*, *37*(20). https://doi.org/10.1029/2010GL044571

Wear, D., & Greis, J. (2002). *Southern Forest Resource Assessment. General Technical Report SRS-53*.

Wei, X., Li, Q., Zhang, M., Giles-Hansen, K., Liu, W., Fan, H., … Liu, S. (2018). Vegetation cover—another dominant factor in determining global water resources in forested regions. *Global Change Biology*, *24*(2), 786–795. https://doi.org/10.1111/gcb.13983

Wieder, W. R., Lawrence, D. M., Fisher, R. A., Bonan, G. B., Cheng, S. J., Goodale, C. L., … Thomas, R. Q. (2019). Beyond Static Benchmarking: Using Experimental Manipulations to Evaluate Land Model Assumptions. *Global Biogeochemical Cycles*, *33*(10), 1289–1309. https://doi.org/10.1029/2018GB006141

Wigley, T., & Jones, P. D. (1985). Influences of precipitation changes and direct CO2 effects on streamflow. *Nature*, *314*(6007), 149–152. https://doi.org/https://doi.org/10.1038/314149a0

Wolf, A., Biondi, F., Hayes, D., Michalak, A. M., Fang, Y., Wei, Y., … Li, J. (2018). Differing ecosystem responses of vegetation cover to extreme drought on the Big Sur coast of California. *Water Resources Research*, *9*(1), 1–14. https://doi.org/10.1117/1.jrs.12.026031

Wuebbles, D. J., Fahey, D. W., Hibbard, K. A., Dokken, D. J., Stewart, B. C., & Maycock, T. K. (2017). Climate science special report: fourth National Climate Assessment. *US Global Change Research Program*, *1*, 470. https://doi.org/10.7930/J0J964J6

Wullschleger, S. D., Post, W. M., & King, A. W. (1995). *n the potential for a CO2 fertilization effect in forests: Estimates of the biotic growth factor based on 58 controlled-exposure studies. In G. M. Woodwell & F. T. Mackenzie (Eds.),*. New York: Oxford University Press, Inc.

Yang, D., Shao, W., Yeh, P. J. F., Yang, H., Kanae, S., & Oki, T. (2009). Impact of vegetation coverage on regional water balance in the nonhumid regions of China. *Water Resources Research*, *45*(7), 1–13. https://doi.org/10.1029/2008WR006948

Yang, Y., Roderick, M. L., Zhang, S., McVicar, T. R., & Donohue, R. J. (2019). Hydrologic implications of vegetation response to elevated CO2 in climate projections. *Nature Climate Change*, *9*(1), 44–48. https://doi.org/10.1038/s41558-018-0361-0

Yue, S., Pilon, P., Phinney, B., & Cavadias, G. (2002). The influence of autocorrelation on the ability to detect trend in hydrological series. *Hydrological Processes*, *16*(9), 1807–1829. https://doi.org/10.1002/hyp.1095

Zeng, Z., Piao, S., Li, L. Z. X., Wang, T., Ciais, P., Lian, X., … Myneni, R. B. (2018). Impact of Earth greening on the terrestrial water cycle. *Journal of Climate*, *31*(7), 2633–2650. https://doi.org/10.1175/JCLI-D-17-0236.1

Zhang, L., Potter, N., Hickel, K., Zhang, Y., & Shao, Q. (2008). Water balance modeling over variable time scales based on the Budyko framework - Model development and testing. *Journal of Hydrology*, *360*(1–4), 117–131. https://doi.org/10.1016/j.jhydrol.2008.07.021

Zhang, Y. K., & Schilling, K. E. (2006). Increasing streamflow and baseflow in Mississippi River since the 1940 s: Effect of land use change. *Journal of Hydrology*, *324*(1–4), 412–422. https://doi.org/10.1016/j.jhydrol.2005.09.033

Zhang, Y. Q., Chiew, F. H. S., Zhang, L., Leuning, R., & Cleugh, H. A. (2008). Estimating catchment evaporation and runoff using MODIS leaf area index and the Penman-Monteith equation. *Water Resources Research*, *44*(10), 1–15. https://doi.org/10.1029/2007WR006563

Zhu, C., & Li, Y. (2014). Long-Term Hydrological Impacts of Land Use/Land Cover Change From 1984 to 2010 in the Little River Watershed, Tennessee. *International Soil and Water*

Conservation Research, *2*(2), 11–21. https://doi.org/10.1016/S2095-6339(15)30002-2

Zhu, Z., Bi, J., Pan, Y., Ganguly, S., Anav, A., Xu, L., … Myneni, R. B. (2013). Global data sets of vegetation leaf area index (LAI)3g and fraction of photosynthetically active radiation (FPAR)3g derived from global inventory modeling and mapping studies (GIMMS) normalized difference vegetation index (NDVI3G) for the period 1981 to 2. *Remote Sensing*, *5*(2), 927–948. https://doi.org/10.3390/rs5020927

Zhu, Z., Piao, S., Myneni, R. B., Huang, M., Zeng, Z., Canadell, J. G., … Zeng, N. (2016). Greening of the Earth and its drivers. *Nature Climate Change*, *6*(8), 791–795. https://doi.org/10.1038/nclimate3004